

1 **Complex response of the CpxAR two-component system to β -lactams on antibiotic**
2 **resistance and envelop homeostasis in *Enterobacteriaceae***

3

4 Muriel Masi^{1,2*}, Elizabeth Pinet^{1,3} and Jean-Marie Pagès^{1*}

5 ¹ UMR_MD1, U-1261, Aix-Marseille Univ, INSERM, IRBA, MCT, Faculté de Pharmacie, 27
6 Boulevard Jean Moulin, 13005 Marseille, France

7 ² Present address: Université Paris Saclay, CEA, CNRS, Institute for Biology of the Cell
8 (I2BC), 91198, Gif-sur-Yvette, France

9 ³ Present address: Selenium Medical, 9049 rue de Québec, 17000 La Rochelle, France

10 *Corresponding authors: muriel.masi@universite-paris-saclay.fr; [saclay.fr](mailto:muriel.masi@i2bc.paris-
11 saclay.fr); jean-marie.pages@univ-amu.fr

12 ORCID iDs: MM <https://orcid.org/0000-0002-1444-7511>; JMP [https://orcid.org/0000-0001-7092-7977](https://orcid.org/0000-0001-
13 7092-7977)

14 **Abstract**

15 The Cpx stress response is widespread among *Enterobacteriaceae*. We have previously
16 reported a mutation in *cpxA* in a multidrug resistant strain of *Klebsiella aerogenes* isolated from
17 a patient treated with imipenem. This mutation yields to a single amino acid substitution
18 (Y144N) located in the periplasmic sensor domain of CpxA. In this work, we sought to
19 characterize this mutation in *Escherichia coli* by using genetic and biochemical approaches.
20 Here, we show that *cpxA*^{Y144N} is an activated allele that confers resistance to β -lactams and
21 aminoglycosides in a CpxR-dependent manner, by regulating the expression of the OmpF porin
22 and the AcrD efflux pump, respectively. We also demonstrate the intimate interconnection
23 between Cpx system and peptidoglycan integrity on the expression of an exogenous AmpC β -
24 lactamase by using imipenem as a cell wall active antibiotic or inactivation of penicillin-binding
25 proteins. Moreover, our data indicate that the Y144N substitution abrogates the interaction
26 between CpxA and CpxP and increase phosphotransfer activity on CpxR. Because the addition
27 of a strong AmpC inducer such as imipenem is known to causes abnormal accumulation of
28 mucopeptides (disaccharide-pentapeptide, *N*-acetylglucosamyl-1,6-anhydro-*N*-acetylmuramyl-
29 L-alanyl-D-glutamy-*meso*-diaminopimelic-acid-D-alanyl-D-alanine) in the periplasmic space,
30 we propose these molecules activate the Cpx system by displacing CpxP from the sensor
31 domain of CpxA. Altogether, these data could explain why large perturbations to peptidoglycan
32 caused by imipenem lead to mutational activation of the Cpx system and bacterial adaptation
33 through multidrug resistance. These results also validate the Cpx system, in particular the
34 interaction between CpxA and CpxP, as a promising therapeutic target.

35

36 **Importance**

37 Cell wall biogenesis is the target of β -lactams, which are potent antibiotics for treating
38 infections caused by Gram-negative bacteria. Resistance to β -lactams is increasing, particularly

39 enteric species such *Klebsiella* and *Enterobacter* spp., both members of the ESKAPE group of
40 problematic clinical pathogen. As a first step to better understand resistance emerged in these
41 organisms, we performed comparative genomics on series of clinical strains of *K. aerogenes*.
42 This allowed in the identification of a number of mutations, all located in genes involved in
43 envelope permeability control. Here, we characterized a gain-of-function mutation in the sensor
44 kinase CpxA. CpxAR is a two-component system that senses and responds to envelope stress.
45 Importantly, characterization of this mutation revealed that the cell wall recycling pathway
46 plays an important role in the resistance of this species when exposed to cell wall-targeting
47 antibiotics.

48 **Introduction**

49 The envelope of Gram-negative bacteria is a complex multilayered structure that is essential for
50 cell viability and provides a protective barrier against environmental stresses. This structure
51 consists of the inner and outer membranes, which are separated by the periplasmic space
52 containing the cell wall or peptidoglycan (PG). PG is a covalently linked scaffold of glycan
53 chains and short peptides that maintains the cell shape and resists against osmotic stress (1). It
54 also provides an oxidizing environment where extracytoplasmic proteins can be stabilized by
55 disulfide bonds (2). PG is synthesized and modified throughout the cell cycle by penicillin
56 binding proteins (PBPs), including high-molecular-weight (HMW) PBPs, which polymerize
57 and crosslink the glycan chains, and low-molecular-weight (LMW) PBPs, often referred to as
58 PG hydrolases, which remodel existing chains (1). In *Escherichia coli* and closely related
59 *Enterobacteriaceae*, the majority of LMW PBPs are D,D-carboxypeptidases — PBPs 5 and 6
60 and DacD that remove the terminal D-alanine from the pentapeptide chains — and/or
61 endopeptidases — PBPs 4 and 7 and AmpH that cleave the peptide side chains and disconnect
62 the glycan polymers (1). While HWM PBPs are essential (3), LMW PBPs are dispensable in
63 standard laboratory conditions (4).

64 Bacteria have evolved sophisticated strategies to monitor and maintain the integrity of their
65 envelope. In *E. coli*, several signal transduction pathways sense envelope alterations in the
66 periplasm and control the expression of adaptive genes (5-9). One of these pathways is Cpx, a
67 two-component system that consists of the transmembrane sensor kinase CpxA and the
68 cytoplasmic response regulator CpxR. Although the molecular characteristics of the inducing
69 signal(s) are unknown, activation of CpxA leads to autophosphorylation at a conserved histidine
70 residue and phosphate transfer to a conserved aspartate in CpxR, which then remodels gene
71 expression (10-13). Divergently transcribed from *cpxAR* is *cpxP*, which encodes a periplasmic
72 protein that negatively modulates the activity of the Cpx system by interacting with the

73 periplasmic sensor domain (SD) of CpxA (14-16). The Cpx system was initially recognized to
74 mediate adaptation to protein misfolding in the periplasm since the first identified genes of the
75 Cpx regulon encoded envelope protein folding and degradation factors such as the
76 protease/chaperone DegP, the peptidyl-prolyl isomerase PpiA and the disulfide oxidase DsbA
77 (12, 17-19). Recent studies have linked the Cpx system to a wider range of other signals and
78 adaptations (20-25), including the detection and repair of perturbations to the PG. First, the Cpx
79 response is activated by the simultaneous deletion of LMW PBPs, resulting in the
80 downregulation of flagellar genes and mobility defects (24). Second, genes of the Cpx regulon
81 are upregulated in the presence of cell wall active antibiotics such as β -lactams (25). Third, Cpx
82 controls the expression of PG-modifying enzymes such as the LdtD (YcbB) transpeptidase (11,
83 22, 23), which catalyzes unusual 3 \rightarrow 3 crosslinks and mediate resistance to β -lactams (26).

84 We have previously reported a *cpxA* mutation in a clinical strain of *K. aerogenes* isolated from
85 a patient with imipenem, a potent β -lactam antibiotic. This strain presented high-level β -lactam
86 resistance associated with the loss of outer membrane porins and an increased β -lactamase
87 activity (27). This mutation yields to a single amino acid substitution (Y144N) located in CpxA-
88 SD. In this work, we characterized CpxA^{Y144N} as a gain-of-function CpxA* mutant.

89 Biochemical analyses showed that this mutation abrogates the interaction between CpxA-SD
90 and CpxP that normally keeps the system in a resting state in the absence of an inducing stress.
91 Accordingly, it increases phosphotransfer events between CpxA and CpxR. Phenotypic
92 analyses showed it conferred resistance to aminoglycosides and β -lactams by acting on
93 identified Cpx regulon members. We also found that cell wall damage is able induce AmpC in
94 a Cpx-dependent manner, suggesting an intimate interconnection between these two pathways.

95 **Materials and Methods**

96

97 **Strains, media and plasmids**

98 Bacterial strains and plasmids used this study are listed in a Supplementary Table. Unless
99 otherwise specified, all assays were performed in the parental strain *E. coli* MC4100 (28).
100 Single-gene-deleted strains were obtained from the KEIO collection (29), and provided by GE
101 Healthcare Dharmacon. Deletions marked with kanamycin resistance cassettes flanked by FRT
102 sites were introduced into MC4100 by P1 transduction and cured by using the FLP helper
103 plasmid pCP20 for serial deletions (30). Genomic DNA of appropriate bacterial strains was
104 prepared with the Wizard ® Genomic DNA purification kit (Promega) according to the
105 manufacturer's protocol. Construction of plasmids was performed by using the In-Fusion ® HD
106 Cloning kit (Clontech) according to the manufacturer's instructions. Point mutations in the
107 *cpxA* gene were generated with the QuickChange II XL site-directed mutagenesis kit
108 (Stratagen) according to the manufacturer's protocol. Oligonucleotides were provided by MWG
109 Eurofins. Cloned DNA inserts were sequenced to confirm the presence of engineered mutations
110 and the absence of other PCR generated mutations (MWG Eurofins). Bacteria were routinely
111 grown at 30 or 37°C in Luria-Bertani (LB) broth or agar (Difco). When needed, ampicillin (100
112 µg/ml); chloramphenicol (30 µg/ml), kanamycin (50 µg/ml), L-arabinose (0.02-0.2%) or IPTG
113 (1 mM) were added. All chemicals were purchased from Sigma.

114

115 **β-galactosidase assays**

116 β-galactosidase activity was assayed on late log-phase bacterial cultures as described by Miller
117 (31). Experiments were independently repeated at least three times.

118

119 **Antibiotic sensitivity assay**

120 Strains susceptibility was determined by efficiency of plating (EOP). Strains containing the
121 empty pBAD33 or *cpxA* derivative plasmids were first induced for 2 h at 37°C with L-arabinose,
122 then serially diluted and plated onto LB agar plates supplemented with antibiotics.
123 Aminoglycosides were amikacin (AMK, 3 µg/ml) and gentamycin (GEN, 5 µg/ml); β-lactams
124 were ceftazidime (CAZ, 0.125 µg/ml) and imipenem (IMP, 0.25 µg/ml); others were
125 fosfomycin (FOF); norfloxacin (NFX, 0.05 µg/ml); erythromycin (ERY, 5 µg/ml). EOP assays
126 were independently repeated at least three times.

127

128 **Overexpression and purification of CpxR-His**

129 A single colony of BL21(DE3) transformed with pET24a+*-cpxR-His* was grown overnight at
130 37°C. The next day, the strain was subcultured 1:100 until reaching an OD₆₀₀ of 0.4 and protein
131 expression was induced with 1 mM IPTG for 3 h at 37°C. The cells were harvested by
132 centrifugation and lysed in 10 mM Tris-HCl, pH 8.0, 150 mM NaCl supplemented with 20 mM
133 imidazole by one passage through a cell disruptor (Constant Systems) at 2 kBars. After removal
134 of the cell debris, CpxR-His in the supernatant was subjected to nickel affinity chromatography
135 by using a HiTrap™ Chelating HP column (GE Healthcare Life Sciences) according to the
136 manufacturer's instructions. Purified CpxR-His protein was passed through a HiTrap™
137 Desalting column (GE Healthcare Life Sciences) to remove imidazole (Figure S1). All protein
138 purification steps were operated by an AKTA protein purification system (Amersham
139 Biosciences).

140

141 **Overexpression of CpxA-His and CpxA^{Y144N}-His and preparation of inner membrane** 142 **vesicles**

143 Single colonies of C41(DE3) transformed with pET24a+*-cpxA-His* or pET24a+*-cpxA^{Y144N}-His*
144 were grown overnight at 37°C. Strains were subcultured 1:100 at 37°C until reaching an OD₆₀₀

145 of 0.4 and protein expression was induced with 1 mM IPTG for 3 h at 30°C. Cells were
146 harvested by centrifugation and lysed in 10 mM Tris-HCl, pH 8.0, 150 mM NaCl by one
147 passage through a cell disruptor (Constant Systems) at 2 kBars. This mainly yields to inside-
148 out inner membrane vesicles (IMVs) (32). After removal of cell debris by low-speed
149 centrifugation ($7,000 \times g$, 20 min, 4°C), the supernatant was ultracentrifuged ($100,000 \times g$, 60
150 min, 4°C) to collect whole-cell envelopes. These were separated into inner and outer
151 membranes by ultracentrifugation through a 30 to 55% (wt/vol) sucrose density gradient as
152 previously described (33). After SDS-PAGE, fractions corresponding inner membranes
153 enriched in CpxA-His or CpxA^{Y144N}-His were pooled, resuspended in phosphorylation buffer
154 (50 mM Tris-HCl, pH 7.5, 10% glycerol (vol/vol), 2 mM dithiothreitol, 50 mM KCl, 5 mM
155 MgCl₂) after removal of sucrose (Figure S2), and used in phosphorylation assays immediately
156 after preparation.

157

158 **Analyzes of CpxA autokinase, kinase and phosphatase activities *in vitro***

159 Purified IMVs containing CpxA-His or CpxA^{Y144N}-His were diluted in phosphorylation buffer
160 at a concentration of approximately 20 mg/ml. Autophosphorylation was tested by using the
161 ADP-Glo™ kinase assay (Promega) according to the manufacturer's instructions (see also
162 supplementary Materials and Methods and Figure S3).

163 For testing kinase and phosphatase activities, CpxA-His and CpxA^{Y144N}-His in IMVs were
164 allowed to autophosphorylate in the presence of ATP, then pelleted by centrifugation and
165 washed twice in phosphorylation buffer to remove residual ATP. For kinase activity assays,
166 CpxR-His was added at a concentration of 1.5 μM (CpxA:CpxR molar ratio ~ 1:3) and
167 incubated for 30 min at room temperature. Purified CpxR-His was labeled with 50 μM acetyl
168 phosphate and used as a positive control (see Supplementary Materials and Methods). All
169 reactions were stopped by the addition of 5 × Laemmli buffer. Phosphoproteins were separated

170 on a 50 μ M Phos-tagTM (Wako Laboratory Chemicals) 12%-PAGE in the presence of 100 μ M
171 $MnCl_2$ and detected by staining with Coomassie Blue R250. For phosphatase activity assays,
172 CpxR~P (from acetyl phosphate labeling) was added and mixtures were incubated for 30
173 minutes at room temperature. Released phosphate levels were measured by using the phosphate
174 colorimetric assay kit (Sigma) according to the manufacturer's instructions (see also
175 Supplementary Materials and Methods and Figure S4).

176

177 **Phos-tag analysis of the CpxR phosphorylation *in vivo***

178 The presence of phosphorylated CpxR (CpxR~P) in lysates of BL21(DE3) co-transformed with
179 pET24a+*-cpxR-His* and pBAD33-*cpxA* or pBAD33-*cpxA*^{Y144N} was assessed by coupling Phos-
180 tagTM PAGE to immunoblotting with HRP-conjugated 6-His Epitope Tag monoclonal antibody
181 (1:2,000) (Sigma). For this, single bacterial colonies were grown overnight at 37°C. The next
182 day, the strains were subcultured 1:100 until reaching an OD₆₀₀ of 0.4. CpxA expression was
183 first induced with 0.2% L-arabinose during 2 h at 37°C, then 1 mM IPTG was added to induce
184 CpxR-His expression for another 3 h at 37°C. 2×10^9 cells were harvested by centrifugation and
185 cell pellets were vigorously resuspended in 1.2 M formic acid. Whole-cell lysates were
186 solubilized by the addition of 5 \times Laemmli buffer and neutralized by the addition of 5 M NaOH.
187 Samples (10 μ l equivalent to 0.2 OD units) were loaded and separated on a 25 μ M Phos-tagTM
188 (Wako Laboratory Chemicals) 12%-PAGE in the presence of 50 μ M $MnCl_2$. Before transfer
189 onto a PVDF membrane, the gel was washed with transfer buffer supplemented with 1 mM
190 EDTA for 10 min to remove excess of $MnCl_2$.

191

192 **Bacterial two-hybrid assay**

193 The interactions between CpxA-SD and CpxP were studied by using a bacterial adenylate
194 cyclase two hybrid (BATCH) assay (Euromedex). The target proteins CpxA and CpxP of *K.*

195 *aerogenes* were separately fused to the C- termini of the T25 and T18 domains, respectively,
196 as previously described (14). To estimate the interaction between CpxA and CpxP, DHM1 *cya*
197 cells were transformed with the recombinant plasmids pKT25-*cpxA/cpxA*^{Y144N}, and pUT18C-
198 *cpxP*. For detection of lactose metabolizing clones, bacteria were grown overnight at 30°C. The
199 next day, 10 µl of each culture was spotted onto LB agar supplemented with 5-bromo-4-chloro-
200 3-indolyl-β-D-galactopyranoside (Xgal, 40 µg/ml) and 0.5 mM IPTG, and incubated for 24 h
201 at 30°C. DHM1 cells were transformed with pKT25-*zip* and pUT18C-*zip* as a positive control
202 (Blue, Lac⁺), and with empty pKT25 and pUT18C plasmids as a negative control (White, Lac⁻).

203

204 **Other protein methods**

205 Whole cell envelopes were prepared as described above and resuspended in 20 mM HEPES-
206 NaOH buffer (pH 7.2). All samples were diluted in Laemmli buffer and heated for 5 min at
207 100°C before loading. Samples corresponding to 0.2 OD units were separated on 10% SDS-
208 PAGE. To better resolve OmpF and OmpC 4 M urea was added to the running gel. Proteins
209 were either visualized after staining with Coomassie Brilliant Blue R250 or transferred onto
210 PVDF Blotting membranes (Bio Rad) as described (27). Protein quantification was performed
211 by using a Pierce™ BCA Protein Assay Kit (Thermo Fisher Scientific) according to the
212 manufacturer's protocol.

213

214 **Quantification of AmpC β-lactamase activity**

215 β-lactamase activity was assessed by using a microtiter plate nitrocefin hydrolysis assay as
216 previously described (34). All chemicals were from Sigma, excepting nitrocefin (Merck) and
217 IMP (Sequoia chemicals Ltd.).

218

219 **Statistical analyses**

220 All assays were repeated at least three times. Results are presented on the basis of the calculated
221 means with standard deviations. When appropriate, *P*-values were calculated and indicated with
222 asterisks as followed: *** $P \leq 0.01$, ** $0.01 < P \leq 0.05$, * $0.05 < P \leq 0.1$.

223 **Results**

224

225 ***cpxA*^{Y144N} is an autoactivated *cpxA* allele (*cpxA*^{*}) that confers antibiotic resistance to β-**
226 **lactams and aminoglycosides**

227 In a previous study, we have reported the evolution of antibiotic resistance in four *K. aerogenes*
228 strains, which were sequentially isolated during the clinical course of a patient under treatment
229 with imipenem. Comparative genomics of these isolates — herein referred as to P1 to P4 —
230 showed that P4 carried mutations in *omp36* (encoding the *E. coli* OmpC ortholog), leading to a
231 premature stop codon, and in *cpxA*, producing a Y144N substitution located in CpxA-SD.
232 Interestingly, we observed that P4 did not produce Omp35 (the *E. coli* OmpF ortholog),
233 although the gene sequence was not altered, and presented increased β-lactamase activity,
234 which could both contribute to high level β-lactam resistance in this strain (27). In order to
235 elucidate the specific effects of the *cpxA*^{Y144N} mutation on antibiotic resistance, wild-type *cpxA*
236 and *cpxA*^{Y144N} were amplified from *K. aerogenes* G7 and P4, respectively, cloned into the
237 pBAD33 plasmid under the control the *P_{ara}* arabinose inducible promoter and expressed in *E.*
238 *coli* K12 MC4100 Δ *ara174*. Several gain-of-function *cpxA*^{*} mutations have been previously
239 isolated and characterized. Among these, *cpxA104*(R33C) and *cpxA101*(T253P) were generated
240 by site-directed mutagenesis and used as positive controls (13). The effects of the CpxA mutants
241 as well as that of the overexpression of the lipoprotein NlpE, a well-characterized Cpx-inducing
242 cue (35), were tested on a chromosomal *ppiA-lacZ* fusion whose activity directly depends on
243 the CpxAR system (17, 36). Consistent with previous results, *ppiA::lacZ* activity increased 2-3
244 fold in response to the overexpression of NlpE, CpxA^{R33C} and CpxA^{T253P}. Similar activation
245 was observed when the CpxA^{Y144N} but not wild-type CpxA was overexpressed, suggesting that
246 *cpxA*^{Y144N} is a new constitutively activated *cpxA*^{*} allele (Figure 1).

247

248 **Antibiotic resistance of *cpxA** mutants is due to specific activation of CpxR**

249 Several recent works suggested that the CpxAR is involved in antibiotic resistance and
250 laboratory and clinical strains of enterobacteria (11, 22, 37-41). Null mutations of *cpxA* — thus
251 lacking both kinase and phosphatase activities — have been shown to activate the Cpx response
252 resulting from the phosphorylation of CpxR by small molecule phosphodonors and to protect
253 cells against external stress caused by hydroxyurea and aminoglycosides (42, 43). Here, we
254 took advantage of the dominant effect of the plasmid-expressed *cpxA** mutations to analyze
255 their effect on antibiotic resistance by using an efficiency of plating assay in a wild-type
256 background. Compared with the empty plasmid or wild-type *cpxA*, *cpxA** mutations conferred
257 some resistance to several antibiotic classes including β -lactams, aminoglycosides and
258 fosfomycin, but not to fluoroquinolones and macrolides (Figures 2A and S5).

259 *cpxA** mutations could cause pleiotropic effects resulting from the phosphorylation of
260 heterologous response regulators other than CpxR. We eliminated this possibility by showing
261 that antibiotic resistance is abolished when a *cpxR* null mutation is introduced in the presence
262 the of a *cpxA*^{Y144N} allele (Figure 2B). Altogether, these results demonstrate that antibiotic
263 resistance conferred by the Cpx response is due to specific phosphorylation of CpxR and
264 concomitant changes in the expression of genes that belong to the Cpx regulon.

265

266 **Multiple Cpx regulon members may be responsible for antibiotic resistance**

267 Having clarified the relationship between the Cpx response and antibiotic resistance, we sought
268 to identify Cpx regulon members responsible for this phenotype by using a candidate approach.
269 This consists in generating null mutants of genes that are known to be up-regulated by Cpx or
270 overproducing genes that are known to be down-regulated by Cpx, then looking for a decrease
271 in resistance in the presence of *cpxA**. AcrD is an inner membrane efflux pump that functions
272 with outer membrane TolC to expel aminoglycosides (44). EOP assays showed that disruption

273 of *acrD* or *tolC* decreased resistance to aminoglycosides in a *cpxA** background, suggesting
274 that resistance to this class of antibiotics is somehow attributable to an elevated expression of
275 *acrD* (Figures 3A). Activation of Cpx decreases *ompF* expression. This occurs at directly at the
276 transcriptional level through the binding of CpxR~P to *ompF* promoter and indirectly through
277 the activation of MzrA that connects CpxAR to EnvZ-OmpR (11, 12, 36, 45). We confirmed
278 the effect of Cpx activation on porin expression by Western blot analysis of whole cell lysates
279 after transient overproduction of NlpE or CpxA* (Figure 3B). In addition, EOP assays showed
280 that plasmid-expression of Omp35, the OmpF ortholog of *K. aerogenes*, decreased resistance
281 to β -lactams but not to aminoglycosides in a *cpxA** background (Figure 3C). Interestingly, the
282 replacement of OmpF to OmpC is often associated with an increased resistance to β -lactams in
283 clinical isolates of problematic enteric bacteria such as *K. aerogenes* and *K. pneumoniae* (27,
284 46, 47). These data suggest that OmpF is the preferred route for the uptake of β -lactams and
285 that the Cpx-dependent inhibition of *ompF* expression is responsible for resistance to this class
286 of antibiotics. Although not tested here, Kurabayashi and colleagues showed that activation of
287 Cpx down-regulated *glpT* and *uhpT*, which encode transporters for fosfomycin together with
288 their native substrates glycerol-3-phosphate and glucose-6-phosphate (39).

289

290 ***In vitro* and *in vivo* biochemical characterization of CpxA^{Y144N}**

291 Like many bacterial sensor kinases, CpxA possesses three enzymatic activities that are critical
292 for signal transduction: autokinase, response regulator kinase and phosphorylated response
293 regulator phosphatase (8). To compare the *in vitro* biochemical activities of CpxA to that of
294 CpxA^{Y144N}, we used IMVs enriched in CpxA-His or CpxA^{Y144N}-His. Autokinase activity was
295 quantified using the ADP-GloTM kinase assay. This assay is performed in two steps: after the
296 kinase reaction in the presence of ATP, the ADP-GloTM reagent is added to terminate the kinase
297 reaction and deplete the remaining ATP then the kinase detection reagent is added to convert

298 ADP into ATP. Newly synthesized ATP is measured using a luciferase/luciferin reaction. The
299 light generated correlates to the amount of ADP generated in the kinase assay, which is
300 indicative of the kinase activity. When the two proteins were incubated with ATP, similar levels
301 of ADP were generated (Figure 4A). This indicated that both proteins catalyze
302 autophosphorylation and that the Y144N substitution does not modify the autokinase activity.
303 Kinase activities were tested by using IMVs and purified CpxR-His. Phosphorylated CpxR was
304 visualized by using the Phos-tag™ PAGE system. CpxR can be phosphorylated *in vitro* by
305 small phosphodonor molecules such as acetyl phosphate (48) and used as a positive control
306 (Figure 4B). However, the Y144N substitution does not increase kinase activity of CpxA on
307 CpxR. Phosphatase activities were tested by using IMVs and phosphorylated CpxR-His.
308 However, similar amounts of phosphate were measured by using a phosphate colorimetric
309 assay. (Figure 4C). Altogether, results from *in vitro* assays suggest CpxA and CpxA^{Y144N}
310 behave similarly.

311 Overproduction of the small periplasmic CpxP protein inhibits the Cpx response and prevents
312 Cpx activation (49). This effect depends on an intact SD as *cpxA24*, which encodes a variant of
313 CpxA lacking 32 amino acids in its periplasmic loop, is a strong *cpxA** allele (13). It has been
314 shown that CpxP interacts with CpxA-SD in unstressed cells and that CpxP inhibits CpxA
315 autophosphorylation in reconstituted proteoliposomes by direct interaction (14, 16). A peptide
316 array indicated that the C-terminal region of CpxA-SD
317 (E₁₃₈DNYQLYLIRPASSSSQSDEINLLFD₁₆₂) might play an important role for the interaction
318 with CpxP (15). Because this region comprises Y144 (underlined), we investigated the impact
319 of the Y144N substitution on the ability of CpxA-SD to interact with CpxP using a bacterial
320 two-hybrid assay (BACTH). BACTH is based on the functional complementation of the T18
321 and T25 domains of the adenylate cyclase of *Bordetella pertussis*, resulting in cAMP synthesis
322 and activation of the lactose operon in an appropriate adenylate cyclase deficient reporter strain

323 (50). A previous study showed efficient interaction when CpxA-SD (P₂₈-P₁₆₄) and signal
324 sequenceless CpxP were fused to the N- or the C-termini of T25 and T18 domains (14). Here,
325 *E. coli* DHM1 was co-transformed with CpxP-T18 and T25-CpxA-SD or T25-CpxA^{Y144N}-SD
326 and transformants were tested for their ability to metabolize Xgal on supplemented LB plates.
327 Co-expression of CpxP-T18 and T25-CpxA-SD but not T25-CpxA^{Y144N}-SD showed blue
328 colonies (Figure 4D). This suggests that the Y144N substitution disrupts the interaction with
329 CpxP and likely explains the constitutive activation of *cpxA*^{Y144N} *in vivo*. In order to confirm
330 this, we analyzed the phosphorylation status of CpxR in intact *E. coli* BL21(DE3) co-
331 transformed with pBAD33-*cpxA* or pBAD33-*cpxA*^{Y144N} and pET24a+-*cpxR*-His by using the
332 Phos-tag PAGE system and immunoblotting with anti-His antibodies. Here, phosphorylated
333 CpxR-His could only be detected in cells expressing the mutant but not the wild-type CpxA
334 (Figure 4E).

335

336 **Interplay between the Cpx system, PBPs and the cell-wall active antibiotic imipenem for** 337 **AmpC β-lactamase induction**

338 *Enterobacter* and *Klebsiella* spp. but not *E. coli* encode an inducible chromosomal AmpC β-
339 lactamase (51-53). Although AmpC is produced at very low levels wild-type strains cultured in
340 standard laboratory conditions, its expression is highly inducible in the presence of β-lactams
341 (AmpC inducers) such as cefoxitin and imipenem. The AmpC induction mechanism is complex
342 and involves at least three proteins that are involved in the PG recycling pathway: AmpR
343 (transcriptional regulator of the LysR family), AmpD (a cytoplasmic amidase) and AmpG (an
344 inner membrane permease) (Figure 6) (54-60). In the current model and under non-inducing
345 conditions, muropeptides from normal PG degradation are removed from the cell wall and
346 transported via AmpG into the cytoplasm where they are cleaved by AmpD to generate free
347 peptides and recycled into the cell wall synthesis. Under inducing conditions, AmpD is unable

348 to process high levels of mucopeptides, which interact with AmpR, creating a conformation that
349 activates the transcription of *ampC*. In clinical strains, high level resistance to β -lactams
350 (especially to third-generation cephalosporins) is due to the derepression of *ampC* mainly
351 resulting from *ampD* mutations (59-62). Results described above showed that expression of
352 *cpxA** in *E. coli* provided some resistance to β -lactams but not to the level to that observed in
353 *K. aerogenes* P4, suggesting the presence an additional mechanism. As compared to strains P1-
354 P3, *K. aerogenes* P4 shows an increased (~ 8.5 fold) β -lactamase activity in non-inducing
355 conditions (Figure 5A). This activity was attributed to a derepressed AmpC, as it could be only
356 inhibited by boronic acid (inhibitor of class C β -lactamases such as AmpC) but not by a mixture
357 of tazobactam and clavulanic acid (inhibitors of class A β -lactamases such as TEM-3) (Figure
358 5B). Because previous whole genome analysis did not reveal mutations in *ampD* (27), we
359 examined the effect of the *cpxA*^{Y144N} mutation on the expression of AmpC. The *ampR-ampC*
360 operon from *K. aerogenes* ATCC13048 was cloned into the pACYC184 vector and co-
361 expressed with *cpxA* or *cpxA*^{Y144N} in *E. coli* C41(DE3). Production of CpxA or CpxA^{Y144N} was
362 induced with IPTG for 1 h then cells were treated with imipenem or not. AmpC levels were
363 monitored by using a nitrocefin degradation assay. Although the two strains were responsive to
364 imipenem, the expression CpxA^{Y144N} showed a significant (~ 5 fold) increase in AmpC activity
365 in the absence of imipenem. This suggested that the Cpx system could be an alternative pathway
366 to induce the expression of *ampC*. To test this hypothesis, different genetic backgrounds of *E.*
367 *coli* K12 MC4100 were transformed with pACYC184-*ampRC* and AmpC levels were analyzed
368 as above. As expected, AmpC activity was highly induced in the presence of imipenem in a
369 wild-type background (~ 12 fold activation) (Figure 5D). In contrast, the absence of AmpG or
370 CpxAR decreased AmpC induction to only 3.5-4.5 fold and the triple mutant showed no
371 induction at all, suggesting that both the AmpG permease and the Cpx system are required for
372 a maximal induction (Figure 5D).

373 The parental strain *E. coli* CS109 and the derivative mutant CS448.3 have been described by
374 K. Young and colleagues in a large study that surveyed the impact of PBPs on bacterial motility
375 (24). Interestingly, the simultaneous removal of PBP4, PBP5, PBP7 and AmpH in CS448.3
376 comprised migration as a result of the activation of the Cpx stress response, which inhibits the
377 production of flagellar proteins. Figure 5E shows AmpC activity is increased CS448.3 as
378 compared to that in CS109. In addition, inactivation of *cpxA* in CS448.3 reduces AmpC activity
379 to the level of the parental strain. While *ampG* is still essential for full AmpC induction, this
380 indicates that activation of Cpx is connecting PBP loss and AmpC activation. This is also
381 consistent with studies that previously linked these two events (63, 64). Altogether, these results
382 demonstrate that the inactivation of PBPs, either by gene deletion or by inhibitory interactions
383 with imipenem, can be sensed by the Cpx system in the periplasmic space and that Cpx
384 activation is providing an adapted response through *ampC* induction.

385 **Discussion**

386 Cpx, together with Bae, Rcs, σ^E , and Psp are usually considered as the main envelope stress
387 response systems in *E. coli* (9). There is convincing evidence that these systems, especially
388 Cpx, can sense and respond to cell wall damage, while the molecular signals remain mostly
389 unknown. Here, we provide functional characterization of the first gain-of-function mutation of
390 CpxA, which was identified in multidrug resistant clinical strain of *K. aerogenes* (27). We
391 demonstrated this mutation confers resistance to β -lactams and aminoglycosides by regulating
392 the expression of effector genes involved in their uptake (*ompF*) or extrusion (*acrD*). Together
393 with other previous studies, these data enlighten the role of the Cpx system in antibiotic
394 resistance in laboratory and clinical strains of enterobacteria (11, 22, 37-41). This mutation also
395 shed new light on how Cpx might sense and respond to PG damage induced by β -lactam
396 treatment through *ampC* regulation and a putative positive feedback loop involving the lytic
397 murein transglycosylase Slt (Figure 6).

398 β -lactams are a potent class of antibiotics used for treating infections caused by Gram-negative
399 bacteria. According to the most widely accepted model, cell wall damage that follows β -lactam
400 treatment results from the drug-induced imbalance of the cell wall biosynthesis machinery,
401 between the murein synthetases and hydrolases. β -lactams bind to PBPs with different
402 affinities, thus were considered to have different consequences on cell morphology and viability
403 (65). Noteworthy, carbapenems, including imipenem and meropenem were shown to saturate
404 simultaneously all four essential HMW PBPs (PBP1a, PBP1b, PBP2 and PBP3) as well as
405 LMW PBPs 4, 5 and 6 at low concentrations, leading to rapid cell killing. In an elegant study,
406 Cho et al. showed that β -lactams (mecillinam and cephalexin) induce a toxic malfunctioning of
407 the cell wall biosynthesis machinery, in which Slt acts a quality control enzyme by degrading
408 uncrosslinked glycan chains (66). Interestingly, *slt* belongs to the Cpx regulon (11).

409 Previous transcriptomic studies have revealed that β -lactams lead to the expression of genes
410 controlled by envelope stress response systems. Indeed, β -lactams specifically targeting the
411 essential bifunctional PBPs (PBP1a and PBP1b, cefsulodin) and the monofunctional PBP2
412 (mecillinam), used alone or in combination, increased the expression of genes regulated by the
413 Rcs, Cpx, σ^E , and Bae systems. Interestingly, Rcs was the only response that was activated in
414 all tested conditions, suggesting this system preferentially responds to PG damages as compared
415 to the others (25). A22, a drug that, like mecillinam, targets the cell elongasome, specifically
416 activates the Rcs response in an RcsF-dependent manner (67). In addition, mecillinam or A22
417 — targeting PBP2 or MreB, both part of the elongasome — and cephalexin — targeting PBP3
418 part of the divisome — led to a 2-fold increase in Cpx activation (22). Endogenous signals,
419 such as genetically blocking a critical step in PG synthesis, can also activate envelope stress
420 responses. In *E. coli*, the simultaneous deletion of specific PBPs (PBP4, 5, 6 and AmpH) led to
421 a reduction in motility that was dependent on the activation of both the Cpx and Rcs systems
422 (24). Interestingly, the activation of the Rcs system was dependent on the activation of the Cpx
423 system, but not vice versa, suggesting Cpx acts upstream of Rcs.

424 Many Gram-negative bacteria encode an inducible chromosomal AmpC β -lactamase, produced
425 in response to specific β -lactam treatment such as imipenem or ceftazidime. In enterobacteria,
426 expression of *ampC* is controlled by the transcriptional regulator AmpR (51-53, 56). Mutants
427 defective of the cytoplasmic AmpD amidase involved in normal cell wall recycling overexpress
428 *ampC* even in the absence of inducer (54, 59-62). This and others findings have led to the
429 conclusion that β -lactam treatment generates major cell wall damage resulting in the
430 accumulation of anhydro-disaccharide-pentapeptide in the periplasm, which is transported into
431 the cytoplasm by the AmpG inner membrane permease and converted to anhydro-
432 monosaccharide-pentapeptide, serving as a signal for *ampC* induction (54-60). Cho *et al.*
433 showed that Slt is responsible for the degradation of uncrosslinked nascent PG into anhydro-

434 disaccharide-pentapeptide when cells are treated with β -lactams (66, 68). Moreover, previous
435 studies have shown the importance of Slt on *ampC* induction (69, 70) and the hypersensitivity
436 of *slt*-defective mutants to β -lactams (71). Bridging all these data together makes the Cpx
437 system emerge as a central player in bacterial physiology upon β -lactam treatment. Cpx first
438 senses PG end products arising from the concomitant inactivation of PBPs and degradation by
439 Slt; Cpx tunes an adapted response by modulating the expression of a number of cell wall
440 modifying enzymes. Among these are Slt and LdtD (11, 23). LdtD is one of the five L,D-
441 transpeptidases of *E. coli* that catalyze non-canonical 3 \rightarrow 3 peptide crosslinks. The Cpx-
442 dependent or independent expression of *ldtD* was later shown to substantially increase
443 resistance to β -lactams (22, 26). Although the inactivation of *ldtD* in the *cpxA*^{Y144N} background
444 did not significantly affect bacterial resistance to β -lactams using EOP assays, we cannot rule
445 out that *ldtD* expression was altered. In the near future, analyses of the PG composition in
446 untreated and imipenem-treated wild-type and Δ *slt* cells are necessary to investigate whether β -
447 lactams that induce large and little amounts of AmpC β -lactamase produce the same PG
448 turnover. We have observed that imipenem is able to activate the Cpx response by using a
449 specific *ppiA-lacZ* reporter fusion (Figure S6). Experiments are now needed to investigate a
450 feedback mechanism *in vivo* by using *slt*-defective and -overexpressing cells. Additionally, an
451 *in vitro* assay will be valuable to test Cpx activation and identify the nature of (the) signaling
452 muropeptide(s).

453 According to the proposed membrane topology of CpxA, amino acid Y144 is located in its
454 periplasmic SD (13). We have shown that this mutation produced constitutive phosphorylated
455 CpxR. This most likely results from the loss of the periplasmic interaction between CpxA and
456 CpxP, an accessory inhibitory protein, which holds the system in a resting state in the absence
457 of stress (14-16, 49). One can suspect that imipenem therapy can select gain-of-function *cpxA**
458 mutations that mimics the presence of an inducing cue. It is also possible that activation of the

459 Cpx system is maintained in this background *via* the Slt feedback loop. It has been proposed
460 that Slt inhibitors may be used in combination therapies with β -lactams (70). Similarly,
461 inhibiting Cpx function would be an effective way to keep AmpC β -lactamases silent and
462 preserve the activity of potent β -lactams against clinically problematic enterobacteria.
463

464 **References**

- 465 1. Typas A, Banzhaf M, Gross CA, Vollmer W. 2011. From the regulation of
466 peptidoglycan synthesis to bacterial growth and morphology. *Nat Rev Microbiol*
467 10:123-136.
- 468 2. Merdanovic M, Clausen T, Kaiser M, Huber R, Ehrmann M. 2011. Protein quality
469 control in the bacterial periplasm. *Annu Rev Microbiol* 65:149-168.
- 470 3. Spratt BG. 1975. Distinct penicillin binding proteins involved in the division,
471 elongation, and shape of *Escherichia coli* K12. *Proc Natl Acad Sci U S A* 72:2999-
472 3003.
- 473 4. Denome SA, Elf PK, Henderson TA, Nelson DE, Young KD. 1999. *Escherichia coli*
474 mutants lacking all possible combinations of eight penicillin-binding proteins: viability,
475 characteristics, and implications for peptidoglycan synthesis. *J Bacteriol* 181:3981-
476 3993.
- 477 5. Flores-Kim J, Darwin AJ. 2016. The phage shock protein response. *Annu Rev Microbiol*
478 70:83-101.
- 479 6. Barchinger SE, Ades SE. 2013. Regulated proteolysis: control of the *Escherichia coli*
480 σ (E)-dependent cell envelope stress response. *Subcell Biochem* 66:129-160.
- 481 7. Majdalani N, Gottesman S. 2005. The Rcs phosphorelay: a complex signal transduction
482 system. *Annu Rev Microbiol* 59:379-405.
- 483 8. Raivio TL. 2014. Everything old is new again: an update on current research on the Cpx
484 envelope stress response. *Biochim Biophys Acta* 2014 1843:1529-1541.
- 485 9. Ruiz N, Silhavy TJ. 2005. Sensing external stress: watchdogs of the *Escherichia coli*
486 cell envelope. *Curr Opin Microbiol* 8:122-126.
- 487 10. Raivio TL. 2014. Everything old is new again: an update on current research on the Cpx
488 envelope stress response. *Biochim Biophys Acta* 2014 1843:1529-1541.

- 489 11. Raivio TL, Leblanc SK, Price NL. 2013. The *Escherichia coli* Cpx envelope stress
490 response regulates genes of diverse function that impact antibiotic resistance and
491 membrane integrity. *J Bacteriol* 195:2755-2767.
- 492 12. Price NL, Raivio TL. 2009. Characterization of the Cpx regulon in *Escherichia coli*
493 strain MC4100. *J Bacteriol* 191:1798-17815.
- 494 13. Raivio TL, Silhavy TJ. 1997. Transduction of envelope stress in *Escherichia coli* by the
495 Cpx two-component system. *J Bacteriol* 179:7724-7733.
- 496 14. Tschauner K, Hörnschemeyer P, Müller VS, Hunke S. 2014. Dynamic interaction
497 between the CpxA sensor kinase and the periplasmic accessory protein CpxP mediates
498 signal recognition in *E. coli*. *PLoS One* 9:e107383.
- 499 15. Zhou X, Keller R, Volkmer R, Krauss N, Scheerer P, Hunke S. 2011. Structural basis
500 for two-component system inhibition and pilus sensing by the auxiliary CpxP protein. *J*
501 *Biol Chem* 286:9805-9814.
- 502 16. Fleischer R, Heermann R, Jung K, Hunke S. 2007. Purification, reconstitution, and
503 characterization of the CpxRAP envelope stress system of *Escherichia coli*. *J Biol Chem*
504 282:8583-8593.
- 505 17. Pogliano J, Lynch AS, Belin D, Lin EC, Beckwith J. 1997. Regulation of *Escherichia*
506 *coli* cell envelope proteins involved in protein folding and degradation by the Cpx two-
507 component system. *Genes Dev* 11:1169-1182.
- 508 18. Danese PN, Silhavy TJ. 1997. The sigma(E) and the Cpx signal transduction systems
509 control the synthesis of periplasmic protein-folding enzymes in *Escherichia coli*. *Genes*
510 *Dev* 11:1183-1193.
- 511 19. Cosma CL, Danese PN, Carlson JH, Silhavy TJ, Snyder WB. 1995. Mutational
512 activation of the Cpx signal transduction pathway of *Escherichia coli* suppresses the
513 toxicity conferred by certain envelope-associated stresses. *Mol Microbiol* 18:491-505.

- 514 20. Delhaye A, Collet JF, Laloux G. 2019. A fly on the wall: How stress response systems
515 can sense and respond to damage to peptidoglycan. *Front Cell Infect Microbiol* 9:380.
- 516 21. Guest RL, Raivio TL. 2016. Role of the Gram-negative envelope stress response in the
517 presence of antimicrobial agents. *Trends Microbiol* 24:377-390.
- 518 22. Delhaye A, Collet JF, Laloux G. 2016. Fine-tuning of the Cpx envelope stress response
519 is required for cell wall homeostasis in *Escherichia coli*. *MBio* 7:e00047-16.
- 520 23. Bernal-Cabas M, Ayala JA, Raivio TL. 2015. The Cpx envelope stress response
521 modifies peptidoglycan cross-linking via the L,D-transpeptidase LdtD and the novel
522 protein YgaU. *J Bacteriol* 197:603-614.
- 523 24. Evans KL, Kannan S, Li G, de Pedro MA, Young KD. 2013. Eliminating a set of four
524 penicillin-binding proteins triggers the Rcs phosphorelay and Cpx stress responses in
525 *Escherichia coli*. *J Bacteriol* 195:4415-4424.
- 526 25. Laubacher ME, Ades SE. 2008. The Rcs phosphorelay is a cell envelope stress response
527 activated by peptidoglycan stress and contributes to intrinsic antibiotic resistance. *J*
528 *Bacteriol* 190:2065-2074.
- 529 26. Hugonnet JE, Mengin-Lecreulx D, Monton A, den Blaauwen T, Carbonnelle E,
530 Veckerlé C, Brun YV, van Nieuwenhze M, Bouchier C, Tu K, Rice LB, Arthur M. 2016.
531 Factors essential for L,D-transpeptidase-mediated peptidoglycan cross-linking and β -
532 lactam resistance in *Escherichia coli*. *Elife* 5:e19469.
- 533 27. Philippe N, Maigre L, Santini S, Pinet E, Claverie JM, Davin-Régli AV, Pagès JM, Masi
534 M. 2015. In vivo evolution of bacterial resistance in two cases of *Enterobacter*
535 *aerogenes* infections during treatment with imipenem. *PLoS One* 10:e0138828.
- 536 28. Casadaban MJ. 1976. Transposition and fusion of the lac genes to selected promoters in
537 *Escherichia coli* using bacteriophage lambda and Mu. *J Mol Biol* 104:541-555.

- 538 29. Baba T, Ara T, Hasegawa M, Takai Y, Okumura Y, Baba M, Datsenko KA, Tomita M,
539 Wanner BL, Mori H. 2006. Construction of *Escherichia coli* K-12 in-frame, single-gene
540 knockout mutants: the Keio collection. *Mol Syst Biol* 2:2006-2008.
- 541 30. Datsenko KA, Wanner BL. 2000. One-step inactivation of chromosomal genes in
542 *Escherichia coli* K-12 using PCR products. *Proc Natl Acad Sci U S A* 97:6640-6645.
- 543 31. Miller J. *Experiments in Molecular Genetics*. 1972. Cold Spring Harbor, NY: Cold
544 Spring Harbor Laboratory.
- 545 32. Altendorf KH, Staehelin LA. 1974. Orientation of membrane vesicles from *Escherichia*
546 *coli* as detected by freeze-cleave electron microscopy. *J Bacteriol* 117:888-899.
- 547 33. Misra R, Castillo-Keller M, Deng M. 2000. Overexpression of protease-deficient
548 DegP(S210A) rescues the lethal phenotype of *Escherichia coli* OmpF assembly mutants
549 in a *degP* background. *J Bacteriol* 182:4882-4888.
- 550 34. Pagès JM, Peslier S, Keating TA, Lavigne JP, Nichols WW. 2015. Role of the outer
551 membrane and porins in susceptibility of β -lactamase-producing *Enterobacteriaceae* to
552 ceftazidime-avibactam. *Antimicrob Agents Chemother* 60:1349-1359.
- 553 35. Snyder WB, Davis LJ, Danese PN, Cosma CL, Silhavy TJ. 1995. Overproduction of
554 NlpE, a new outer membrane lipoprotein, suppresses the toxicity of periplasmic LacZ
555 by activation of the Cpx signal transduction pathway. *J Bacteriol* 177:4216-4123.
- 556 36. Gerken H, Charlson ES, Cicirelli EM, Kenney LJ, Misra R. 2009. MzrA: a novel
557 modulator of the EnvZ/OmpR two-component regulon. *Mol Microbiol* 72:1408-1422.
- 558 37. Dean CR, Barkan DT, Bermingham A, Blais J, Casey F, Casarez A, Colvin R, Fuller J,
559 Jones AK, Li C, Lopez S, Metzger LE 4th, Mostafavi M, Prathapam R, Rasper D, Reck
560 F, Ruzin A, Shaul J, Shen X, Simmons RL, Skewes-Cox P, Takeoka KT, Tamrakar P,
561 Uehara T, Wei JR. 2018. Mode of action of the monobactam LYS228 and mechanisms

- 562 decreasing *in vitro* susceptibility in *Escherichia coli* and *Klebsiella pneumoniae*.
563 Antimicrob Agents Chemother 62:e01200-18.
- 564 38. Huang H, Sun Y, Yuan L, Pan Y, Gao Y, Ma C, Hu G. 2016. Regulation of the two-
565 component regulator CpxR on aminoglycosides and β -lactams resistance in *Salmonella*
566 *enterica* serovar Typhimurium. Front Microbiol 7:e604.
- 567 39. Kurabayashi K, Hirakawa Y, Tanimoto K, Tomita H, Hirakawa H. 2014. Role of the
568 CpxAR two-component signal transduction system in control of fosfomycin resistance
569 and carbon substrate uptake. J Bacteriol 196:248-256.
- 570 40. Mahoney TF, Silhavy TJ. 2013. The Cpx stress response confers resistance to some, but
571 not all, bactericidal antibiotics. J Bacteriol 195:1869-1874.
- 572 41. Hu WS, Chen HW, Zhang RY, Huang CY, Shen CF. 2011. The expression levels of
573 outer membrane proteins STM1530 and OmpD, which are influenced by the CpxAR
574 and BaeSR two-component systems, play important roles in the ceftriaxone resistance
575 of *Salmonella enterica* serovar Typhimurium. Antimicrob Agents Chemother 55:3829-
576 3837.
- 577 42. Kohanski MA, Simmons LA, Winkler JA, Collins JJ, Walker GC. 2009. Hydroxyurea
578 induces hydroxyl radical-mediated cell death in *Escherichia coli*. Mol Cell 36:845-860.
579 PubMed PMID: 20005847.
- 580 43. Kohanski MA, Dwyer DJ, Hayete B, Lawrence CA, Collins JJ. 2007. A common
581 mechanism of cellular death induced by bactericidal antibiotics. Cell 130:797-810.
- 582 44. Rosenberg EY, Ma D, Nikaido H. 2000. AcrD of *Escherichia coli* is an aminoglycoside
583 efflux pump. J Bacteriol 182:1754-1756.
- 584 45. Batchelor E, Walthers D, Kenney LJ, Goulian M. 2005. The *Escherichia coli* CpxA-
585 CpxR envelope stress response system regulates expression of the porins OmpF and
586 OmpC. J Bacteriol 187:5723-5731.

- 587 46. Vergalli J, Bodrenko IV, Masi M, Moynié L, Acosta-Gutiérrez S, Naismith JH, Davin-
588 Regli A, Ceccarelli M, van den Berg B, Winterhalter M, Pagès JM. 2019. Porins and
589 small-molecule translocation across the outer membrane of Gram-negative bacteria. Nat
590 Rev Microbiol doi: 10.1038/s41579-019-0294-2.
- 591 47. Lavigne JP, Sotto A, Nicolas-Chanoine MH, Bouziges N, Pagès JM, Davin-Regli A.
592 2013. An adaptive response of *Enterobacter aerogenes* to imipenem: regulation of porin
593 balance in clinical isolates. Int J Antimicrob Agents 41:130-136.
- 594 48. Lukat GS, McCleary WR, Stock AM, Stock JB. 1992. Phosphorylation of bacterial
595 response regulator proteins by low molecular weight phospho-donors. Proc Natl Acad
596 Sci U S A 89:718-722.
- 597 49. Raivio TL, Laird MW, Joly JC, Silhavy TJ. 2000. Tethering of CpxP to the inner
598 membrane prevents spheroplast induction of the Cpx envelope stress response. Mol
599 Microbiol 37:1186-1197.
- 600 50. Karimova G, Pidoux J, Ullmann A, Ladant D. 1998. A bacterial two-hybrid system
601 based on a reconstituted signal transduction pathway. Proc Natl Acad Sci U S A 1998
602 95:5752-5756.
- 603 51. Fisher JF, Mobashery S. 2014. The sentinel role of peptidoglycan recycling in the β -
604 lactam resistance of the Gram-negative *Enterobacteriaceae* and *Pseudomonas*
605 *aeruginosa*. Bioorg Chem 56:41-48.
- 606 52. Wiedemann B, Pfeifle D, Wiegand I, Janas E. 1998. Beta-lactamase induction and cell
607 wall recycling in Gram-negative bacteria. Drug Resist Updat 1:223-226.
- 608 53. Honoré N, Nicolas MH, Cole ST. 1986. Inducible cephalosporinase production in
609 clinical isolates of *Enterobacter cloacae* is controlled by a regulatory gene that has been
610 deleted from *Escherichia coli*. EMBO J 5:3709-3714.

- 611 54. Honoré N, Nicolas MH, Cole ST. 1989. Regulation of enterobacterial cephalosporinase
612 production: the role of a membrane-bound sensory transducer. *Mol Microbiol* 3:1121-
613 1130.
- 614 55. Dietz H, Pfeifle D, Wiedemann B. 1997. The signal molecule for beta-lactamase
615 induction in *Enterobacter cloacae* is the anhydromuramyl-pentapeptide. *Antimicrob*
616 *Agents Chemother* 41:2113-2120.
- 617 56. Jacobs C, Frère JM, Normark S. 1997. Cytosolic intermediates for cell wall biosynthesis
618 and degradation control inducible beta-lactam resistance in Gram-negative bacteria.
619 *Cell* 88:823-832.
- 620 57. Dietz H, Pfeifle D, Wiedemann B. 1996. Location of N-acetylmuramyl-L-alanyl-D-
621 glutamylmesodiaminopimelic acid, presumed signal molecule for beta-lactamase
622 induction, in the bacterial cell. *Antimicrob Agents Chemother* 40:2173-2177.
- 623 58. Jacobs C, Huang LJ, Bartowsky E, Normark S, Park JT. 1994. Bacterial cell wall
624 recycling provides cytosolic muropeptides as effectors for beta-lactamase induction.
625 *EMBO J* 13:4684-4694.
- 626 59. Korfmann G, Sanders CC. 1989. *ampG* is essential for high-level expression of AmpC
627 beta-lactamase in *Enterobacter cloacae*. *Antimicrob Agents Chemother* 33:1946-1951.
- 628 60. Guérin F, Isnard C, Cattoir V, Giard JC. 2015. Complex regulation pathways of AmpC-
629 mediated β -lactam resistance in *Enterobacter cloacae* complex. *Antimicrob Agents*
630 *Chemother* 59:7753-7761.
- 631 61. Kaneko K, Okamoto R, Nakano R, Kawakami S, Inoue M. 2005. Gene mutations
632 responsible for overexpression of AmpC beta-lactamase in some clinical isolates of
633 *Enterobacter cloacae*. *J Clin Microbiol* 43:2955-2958.
- 634 62. Korfmann G, Sanders CC, Moland ES. 1991. Altered phenotypes associated with *ampD*
635 mutations in *Enterobacter cloacae*. *Antimicrob Agents Chemother* 35:358-364.

- 636 63. Pfeifle D, Janas E, Wiedemann B. 2000. Role of penicillin-binding proteins in the
637 initiation of the AmpC beta-lactamase expression in *Enterobacter cloacae*. *Antimicrob*
638 *Agents Chemother* 44:169-172.
- 639 64. Sanders CC, Bradford PA, Ehrhardt AF, Bush K, Young KD, Henderson TA, Sanders
640 WE Jr. 1997. Penicillin-binding proteins and induction of AmpC beta-lactamase.
641 *Antimicrob Agents Chemother* 41:2013-2015.
- 642 65. Satta G, Cornaglia G, Mazzariol A, Golini G, Valisena S, Fontana R. 1995. Target for
643 bacteriostatic and bactericidal activities of beta-lactam antibiotics against *Escherichia*
644 *coli* resides in different penicillin-binding proteins. *Antimicrob Agents Chemother*
645 39:812-818.
- 646 66. Cho H, Uehara T, Bernhardt TG. 2014. Beta-lactam antibiotics induce a lethal
647 malfunctioning of the bacterial cell wall synthesis machinery. *Cell* 159:1300-1311.
- 648 67. Lai GC, Cho H, Bernhardt TG. 2017. The mecillinam resistome reveals a role for
649 peptidoglycan endopeptidases in stimulating cell wall synthesis in *Escherichia coli*.
650 *PLoS Genet* 13:e1006934.
- 651 68. Lee M, Heseck D, Llarrull LI, Lastochkin E, Pi H, Boggess B, Mobashery S. 2013.
652 Reactions of all *Escherichia coli* lytic transglycosylases with bacterial cell wall. *J Am*
653 *Chem Soc* 135:3311-3314.
- 654 69. Korsak D, Liebscher S, Vollmer W. 2005. Susceptibility to antibiotics and beta-
655 lactamase induction in murein hydrolase mutants of *Escherichia coli*. *Antimicrob*
656 *Agents Chemother* 49:1404-1409.
- 657 70. Kraft AR, Prabhu J, Ursinus A, Høltje JV. 1999. Interference with murein turnover has
658 no effect on growth but reduces beta-lactamase induction in *Escherichia coli*. *J Bacteriol*
659 181:7192-7198.

660 71. Templin MF, Edwards DH, Höltje JV. 1992. A murein hydrolase is the specific target
661 of bulgecin in *Escherichia coli*. J Biol Chem 267:20039-20043.

662 **Figure legends**

663 **Figure 1.** *cpxA*^{Y144N} is a *cpxA** allele. Effect of CpxA, CpxA^{Y144N}, CpxA^{R33C}, CpxA^{T252P} and
664 NlpE on *ppiA* expression by assaying β -galactosidase activities of a chromosomal *lacZ* fusions.

665 **Figure 2.** *cpxA** mutations confer resistance to β -lactams, aminoglycosides and fosfomycin.
666 (A) Efficiency of plating (EOP) assay on LB agar plates supplemented with 3 μ g/ml amikacin
667 (AMK), 2.5 μ g/ml gentamicin (GEN), 0.5 μ g/ml imipenem (IMP), 0.125 μ g/ml ceftazidime
668 (CAZ) or 4 μ g/ml fosfomycin (FOF) and grown at 37°C. Susceptibility was determined for the
669 following strains: RAM1292 transformed with pBAD33, pBAD33-*cpxA*, pBAD33-*cpxA*^{Y144N},
670 pBAD33-*cpxA*^{R33C}, or pBAD33-*cpxA*^{T252P}. (B) Deleting *cpxR* in RAM1292 pBAD33-*cpxA*^{Y144N}
671 abolished antibiotic resistance.

672 **Figure 3.** The Cpx response regulates genes that impact antibiotic resistance. (A), (C): EOP
673 assays. (A) Deleting the *acrD* or *tolC* efflux pump components decreased resistance to
674 aminoglycosides in RAM1292 pBAD33-*cpxA*^{Y144N}. (B) OMP expression level is altered by
675 *cpxA*^{Y144N}. RAM1292 transformed with pBAD33, pBAD33-*cpxA*, pBAD33-*cpxA*^{Y144N},
676 pBAD33-*cpxA*^{R33C} and pBAD33-*cpxA*^{T252P} were cultured and induced for 2 h with 0.2% L-
677 arabinose. OMPs were detected from whole cell lysates using polyclonal antibodies directed
678 against OmpF/C/A as described in the Materials and Methods section. Equivalent of 0.2 OD₆₀₀
679 units were loaded per well. OmpF/C levels were normalized using the OmpA intensity signal.
680 (C) Plasmid expression of the OmpF ortholog of *E. aerogenes* Omp35 restores the susceptibility
681 of RAM1292 pBAD33-*cpxA*^{Y144N} to β -lactams.

682 **Figure 4.** Enzymatic activities of CpxA^{Y144N}. (A) CpxA-His and CpxA^{Y144N}-His exhibit similar
683 autophosphorylation activities. Autophosphorylation was tested by using the ADP-Glo™
684 kinase assay on inner membrane fractions as described in the Materials and Methods section.
685 Reactions were performed with 5 μ l IMVs in the presence of 100 μ M or 1 mM ATP for 30 min
686 at room temperature. The two step assay includes the removal of the remaining ATP then the

687 simultaneous conversion the ADP produced by the kinase reaction to ATP and into light by a
688 luciferin/luciferase reaction. Bioluminescent signals are proportional to the ADP produced and
689 the activity of the kinase. The amount of ADP produced from each reaction was calculated by
690 using ATP to ADP standard curves. **(B)** CpxA-His and CpxA^{Y144N}-His exhibit similar *in vitro*
691 kinase activity on CpxR. CpxA-His or CpxA^{Y144N}-His in enriched IMVs (5 μ l) was
692 phosphorylated under standard conditions then incubated in the presence of 1.5 μ M purified
693 CpxR-His for 30 min. Samples were analyzed by using Phos-tagTM PAGE fractionation. **(C)**
694 CpxA-His and CpxA^{Y144N}-His exhibit similar *in vitro* phosphatase activity on CpxR. CpxR-His
695 was phosphorylated with acetyl-phosphate as described in Materials and Methods.
696 Phosphorylated CpxR-His was incubated in the presence of CpxA-His or CpxA^{Y144N}-His
697 enriched IMVs (5 μ l). Phosphate standards and samples (duplicates) were brought to 200 μ l with
698 water in a microplate. 30 μ l of phosphate reagent were added to each well and mixtures were
699 incubated at room temperature in the dark. After 30 min, absorbance at 650 nm was measured.
700 **(D)** Substitution Y144N in the periplasmic sensor domain of CpxA affects binding to CpxP.
701 Protein-protein interaction analysis was performed by using BATCH. CpxP and the sensor
702 domain of the wild-type CpxA or mutant CpxA^{Y144N} (CpxA-SD and CpxA^{Y144N}-SD) were fused
703 to the C- and the N-terminal ends of the T18 and T25 fragments of *B. pertussis* adenylate
704 cyclase, respectively. *E. coli* cells DHM1 co-transformed with plasmids encoding the hybrid
705 proteins were grown overnight, spotted on an Xgal plate and incubated at 30°C for 24 h. **(E)** *In*
706 *vivo* detection of phosphorylated and non-phosphorylated CpxR. *E. coli* BL21(DE3) was co-
707 transformed with pET24+*-cpxR-His* and pBAD33-*cpxA* or pBAD33-*cpxA*^{Y144N}. Cells were
708 grown at 37°C to mid-log phase and protein expression was induced with 0.2% L-arabinose for
709 2 h then 1 mM IPTG for 3 h. Bacteria were pelleted by centrifugation, lysed with formic acid
710 and samples were rapidly fractionated by Phos-tagTM PAGE and blotted with anti-His
711 antibodies.

712 **Figure 5.** Interplay between the Cpx system, PBPs and the cell-wall active antibiotic imipenem
713 for β -lactamase induction. (A)-(D): Nitrocefin degradation assays were performed as described
714 in the Materials and Methods section. (A) *E. aerogenes* clinical strain P4 exhibits high β -
715 lactamase activity. Total β -lactamase activity was assessed in a series of clinical strains of *E.*
716 *aerogenes* (P1 to P4) sequentially isolated from a patient under treatment with IMP. (B) β -
717 lactamase activity in P4 is mainly due to AmpC. Inhibition of the β -lactamase activity in *E.*
718 *aerogenes* P4 and control strains of *E. coli* expressing constitutive TEM-3 or AmpC from a
719 plasmid. Tazobactam/clavulanic acid and boronic acid were used as specific inhibitors of class
720 A (e.g. TEM-3) and class C (e.g. AmpC) β -lactamases, respectively. (C) AmpC activity is
721 increased upon the expression of CpxA^{Y144N} in the absence of IMP. *E. coli* C41(DE3) was co-
722 transformed with pACYC184-*ampRC* and pET24a+*-cpxA-His* or pET24a+*-cpxA^{Y144N}-His*.
723 Expression of the CpxA proteins was induced with 1 mM IPTG for 1 h at 30°C, then cells were
724 exposed or not to IMP (0.32 μ g/ml) for 1 h. (D) Functional AmpG and CpxAR are both required
725 for inducing AmpC activity in response to IMP exposure. (E) Loss of specific PBPs induces
726 AmpC activity in a Cpx-dependent manner. In (D) and (E) *E. coli* MC4100, CS109 and
727 derivative mutants were transformed with pACYC184-*ampRC*, grown and induced as described
728 Materials and Methods. Asterisks indicate that the data determined for the mutant samples are
729 significantly different from those of the wild-type control samples; nd, not determined.

730 **Figure 6.** Schematic representation of the interplay between the Cpx system and the
731 chromosomal AmpC β -lactamase regulatory pathway in *Enterobacteriaceae*. In a wild-type
732 background and under non-inducing conditions, the PG is recycled. PG degradation products
733 (disaccharide-peptides, aD-peptides) are generated in the periplasm by the activity of PBPs.
734 aD-peptides (aD-tripeptides, aD-tetrapeptides and aD-pentapeptides) are transported into the
735 cytoplasm by the inner membrane permease AmpG and processed by the amidase AmpD into
736 their corresponding monosaccharide-peptides (aM-peptides). aM-peptides are then transformed

737 into UDP-MurNAc-pentapeptides and incorporated to the PG biosynthesis pathway to complete
738 the recycling process. In the cytoplasm, these UDP-MurNAc-pentapeptides interact with
739 AmpR, creating a conformation that represses the transcription of *ampC*. In addition, normal
740 interactions between CpxP and the periplasmic sensor domain of CpxA keeps in the Cpx system
741 « Off ». Strong AmpC inducers such as imipenem simultaneously bind to several PBPs; lead to
742 an increase of aD-pentapeptides in the periplasm (AmpG saturation) and of aM-tripeptides
743 (AmpD saturation) in the cytoplasm. In the cytoplasm, the accumulated aM-tripeptides displace
744 UDP-MurNAc-pentapeptides from AmpR, creating a conformation that activates the
745 transcription of *ampC*. In addition, our data showed that the increased level of aD-pentapeptides
746 in the periplasm is sensed by the Cpx system. The release of CpxP from CpxA-SD by competing
747 interactions with aD-pentapeptides probably switches the Cpx system « On ». High level of
748 CpxR~P leads to AmpC overexpression thus to β -lactam resistance. The proposed feedback
749 loop involving the lytic glycosylase appears in red. It also unknown which of CpxA or CpxP
750 interacts with the putative signaling muropeptide in the periplasm. The *cpxA*^{Y144N} mutation
751 alters the interaction between the CpxA-SD and CpxP. This activates the Cpx response and
752 leads to *ampC* overexpression, even in the absence of AmpC inducers. This mutation also acts
753 on other genes of the Cpx regulon that impact antibiotic resistance.

754 **Acknowledgments**

755 We thank Estelle Dumont and Julia Vergalli for fruitful discussions all through this study; Anne
756 Davin-Régli and Jean-Michel Bolla for their critical reading of this manuscript. We also
757 generously thank Kevin D. Young (University of Arkansas for Medical Sciences) and Malcom
758 G. P. Page (Jacobs University Bremen) for sharing strains and plasmids.

759 The authors declare that they have no competing interests.

760 MM and JMP design the research. MM and EP performed the experiments. MM and JMP wrote
761 the paper.

762 The research leading to these results was conducted as part of the TRANSLOCATION
763 consortium and has received support from the Innovative Medicines Initiative Joint
764 Undertaking under Grant Agreement n°115525, resources, which are composed of financial
765 contribution from the European Union's seventh framework program (FP7/2007-2013) and
766 EFPIA companies in kind contribution.

Fig. 1

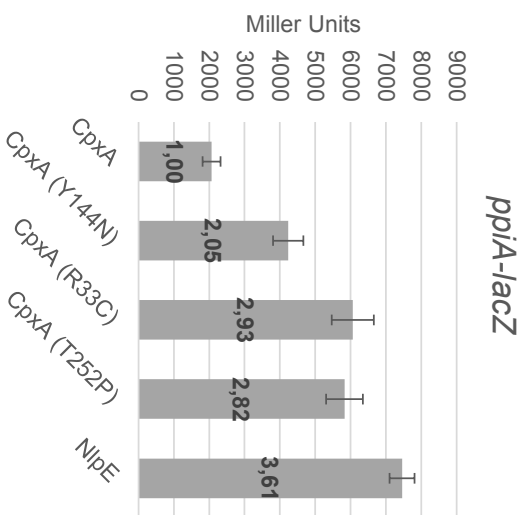


Fig. 2

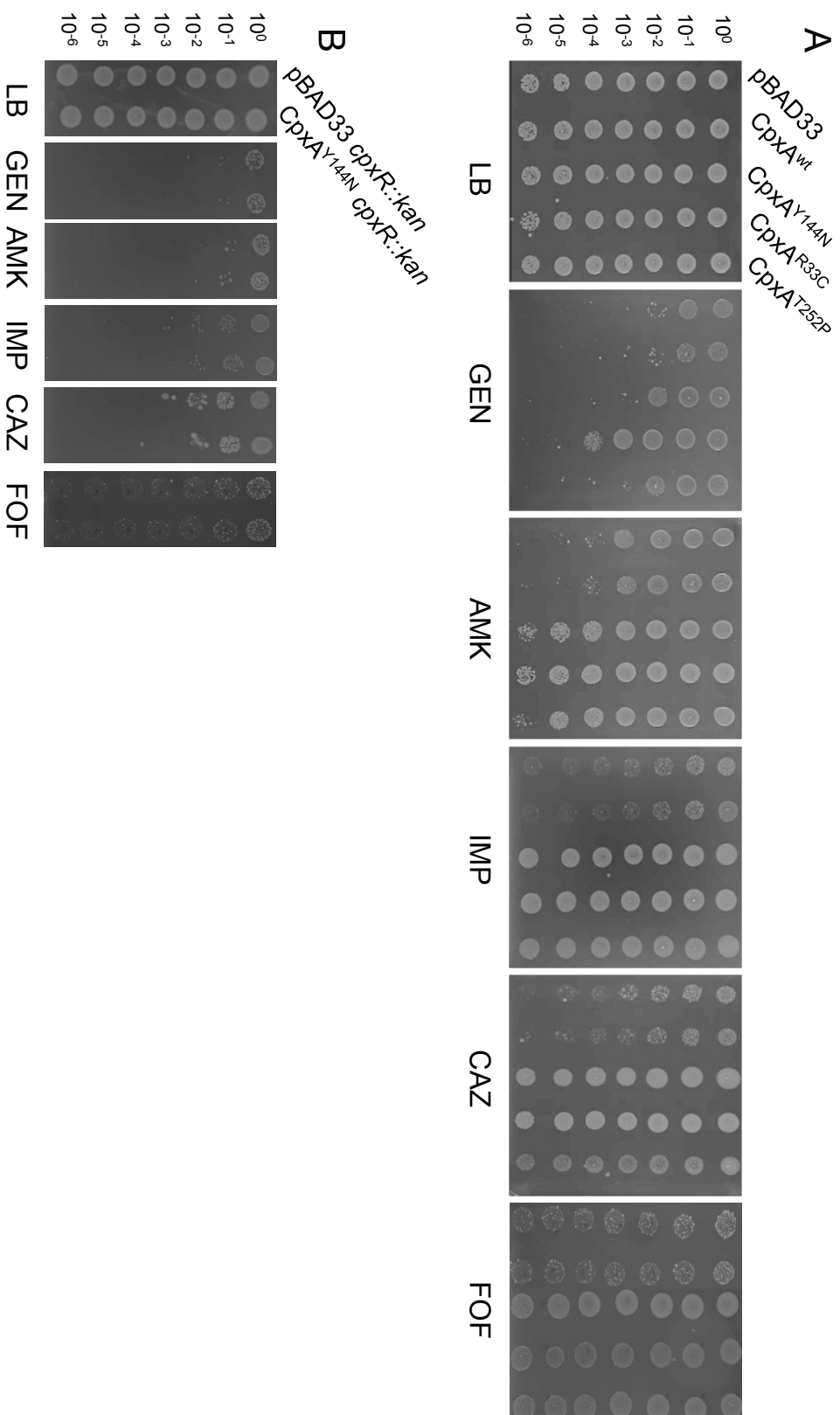


Fig. 3

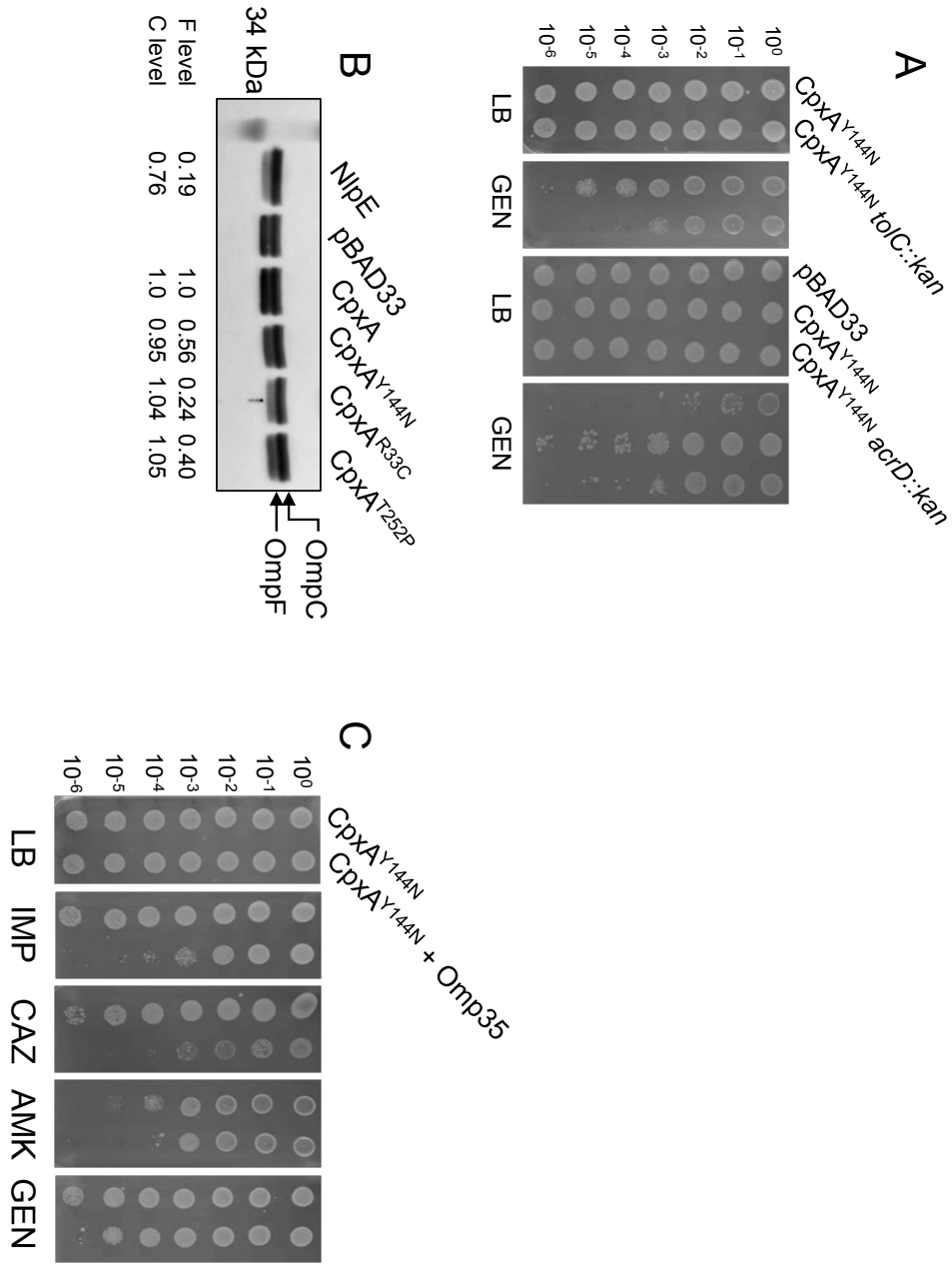


Fig. 4

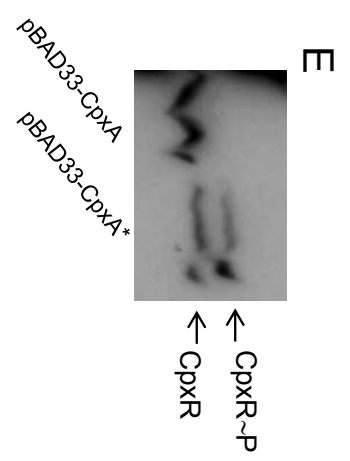
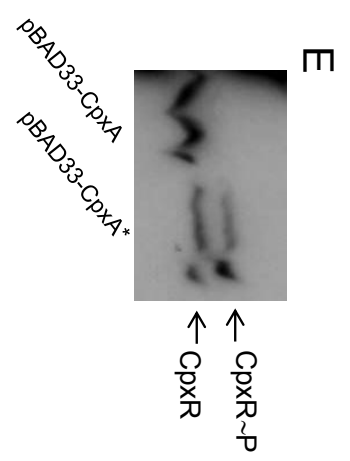
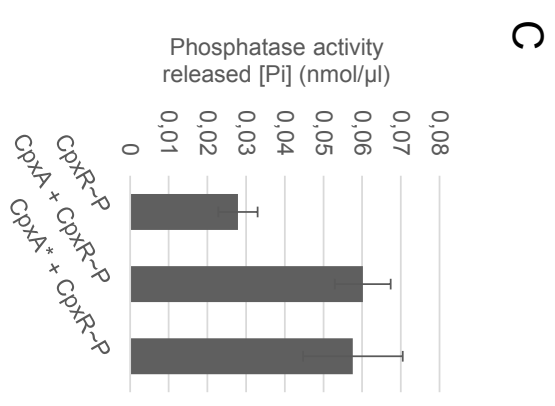
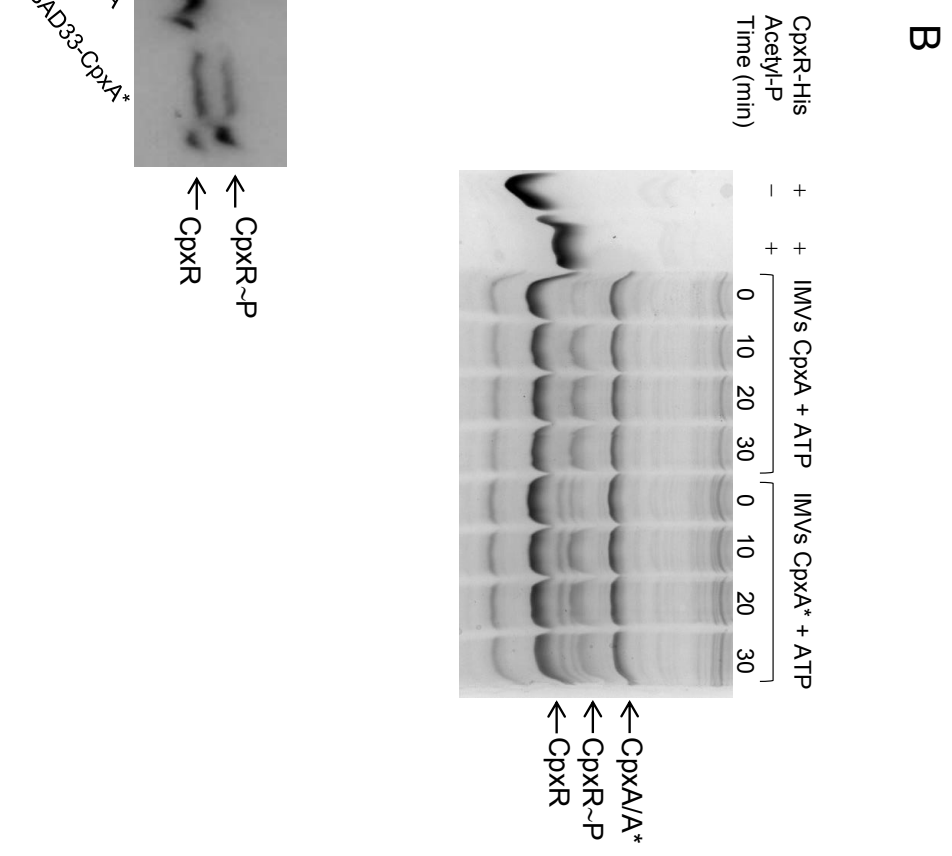
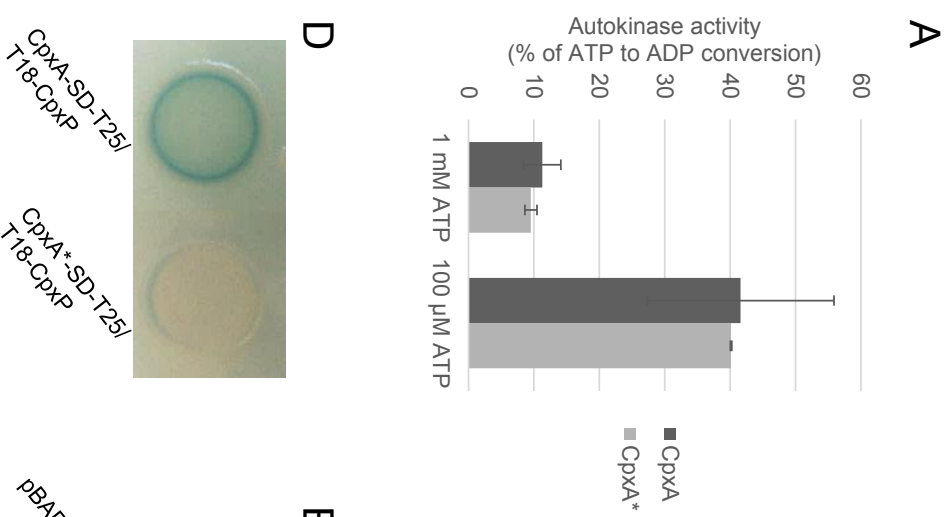
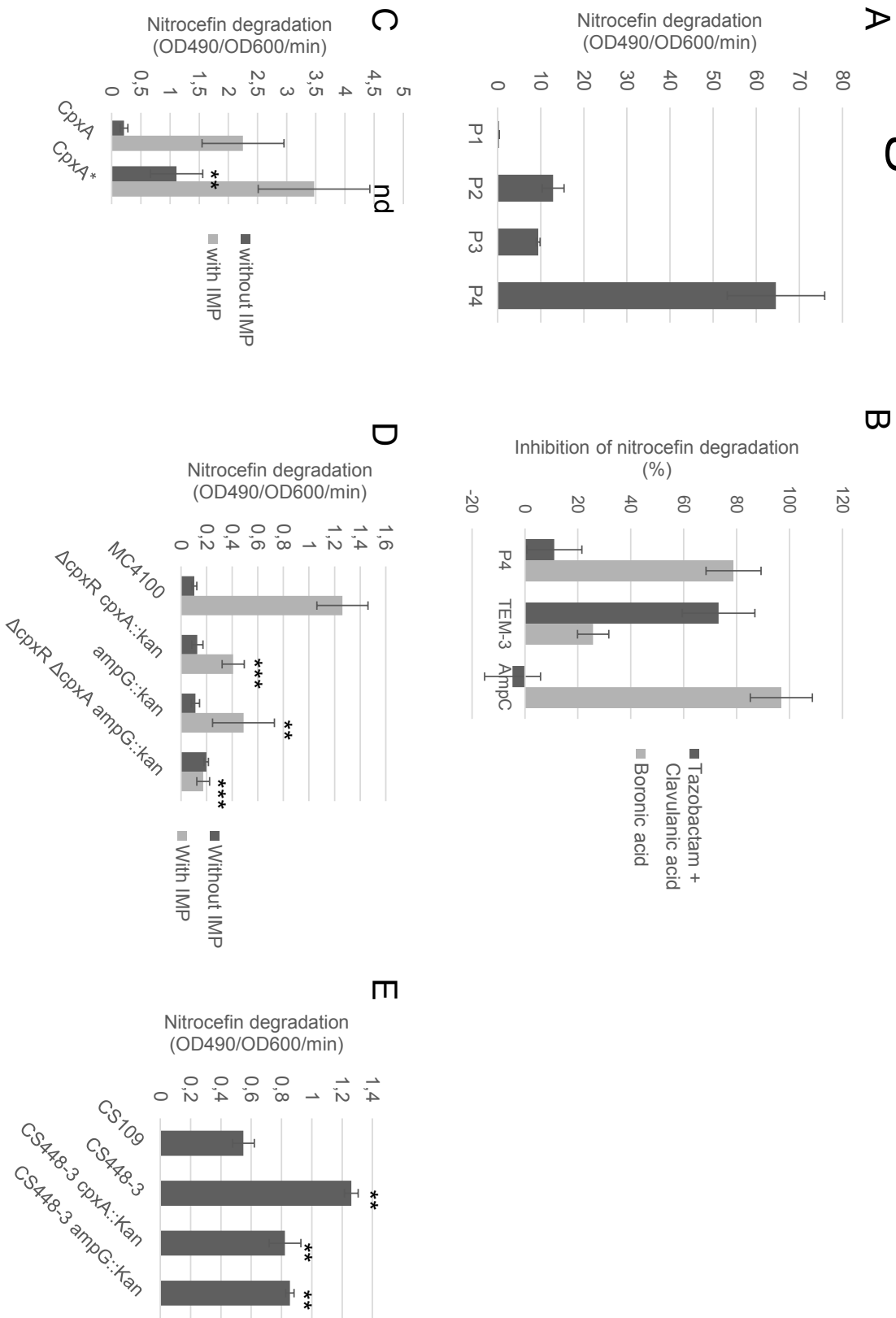


Fig. 5

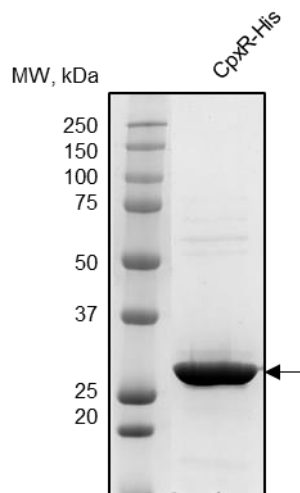


- 1 **Supplementary data**
- 2 **Supplementary Materials and Methods.**
- 3 **Supplementary Table. Bacterial strains and plasmids.**

Strain or plasmid	Relevant characteristics	Reference or source
<i>K. aerogenes</i> strains		
G7	Clinical isolate, source for amplification of <i>cpxA</i> and <i>nlpE</i>	1
P4	Clinical isolate, source of amplification of <i>cpxA</i> ^{Y144N}	1
ATCC13048	Source for amplification of <i>omp35</i> and <i>ampR-ampC</i>	Lab collection
<i>E. coli</i> strains		
MC4100	[<i>araD139</i>] _{B/r} , $\Delta(\argF-lac)169$, λ^- , <i>e14-</i> , <i>flhD5301</i> , $\Delta(\text{fruK-yeiR})725(\text{fruA25})$, <i>relA1</i> , <i>rpsL150</i> (strR), <i>rbsR22</i> , $\Delta(\text{fimB-fimE})632(::\text{IS1})$, <i>deoC1</i>	2
RAM1292	MC4100 ΔaraI74	3
RAM1330	RAM1292 $\Delta\text{tolC}::\text{kan}$	4
RAM1551	RAM1292 $\Delta\text{ppiA-lacZ}$	5
Stellar	Host for cloning, F ⁻ , <i>endA1</i> , <i>supE44</i> , <i>thi-1</i> , <i>recA1</i> , <i>relA1</i> , <i>gyrA96</i> , <i>phoA</i> , $\Phi 80d$ <i>lacZ</i> Δ M15, $\Delta(\text{lacZYA-argF})$ U169, $\Delta(\text{mrr-hsdRMS-mcrBC})$, ΔmcrA , λ^-	CloneTech
BL21(DE3)	Host for protein overexpression, <i>fhuA2</i> [<i>lon</i>] <i>ompT gal</i> (λ DE3) [<i>dcm</i>] ΔhsdS , λ DE3 = λ <i>sBamHI</i> Δ <i>EcoRI-B</i> <i>int::(\text{lacI}::\text{PlacUV5}::\text{T7 gene1})</i> <i>i21</i> Δnin5	Lab collection
C41(DE3)	Host for toxic membrane protein overexpression, derivative of BL21(DE3)	Lab collection
DHM1	Host adenylate cyclase complementation, F ⁻ , <i>cya-854</i> , <i>recA1</i> , <i>endA1</i> , <i>gyrA96</i> (Nal ^r), <i>thi1</i> , <i>hsdR17</i> , <i>spoT1</i> , <i>rfbD1</i> , <i>glnV44</i> (AS)	Euromedex
BW25113	Parental strain of single-gene-deletion, $\Delta(\text{araD-araB})567$, $\Delta\text{lacZ4787}(\text{::rrnB-3})$, λ^- , <i>rph-1</i> , $\Delta(\text{rhaD-rhaB})568$, <i>hsdR514</i>	KEIO collection
BW25113 <i>cpxR::kan</i>	Source for P1 transduction	KEIO collection
BW25113 <i>cpxA::kan</i>	Source for P1 transduction	KEIO collection
BW25113 <i>acrD::kan</i>	Source for P1 transduction	KEIO collection
BW25113 <i>ampG::kan</i>	Source for P1 transduction	KEIO collection
BW25113 <i>ldtD::kan</i>	Source for P1 transduction	KEIO collection
CS109	W1485 <i>rph-1 katF</i> (<i>rpoS</i>)	6
CS448-3	CS109 <i>dacB::res dacA::res pbpG::res ampH::res</i>	7
Plasmids		
pCP20	<i>cI857 repA</i> (Ts) P _R : <i>flp</i> Amp ^r Cam ^r	8
pAD7	Constitutive AmpC	Gift from MGP. Page
pTEM-3	TEM-3	Gift from MGP. Page
pBAD24	Amp ^r ; Expression vector; <i>P</i> _{ara} arabinose inducible	9
pBAD24- <i>nlpE</i>	NlpE of <i>K. aerogenes</i> G7 cloned into pBAD24	This study
pBAD24- <i>omp35</i>	Omp35 of <i>K. aerogenes</i> ATCC13048 cloned into pBAD24	This study

pBAD33	Cm ^r ; Expression vector; <i>P_{ara}</i> arabinose inducible	9
pBAD33- <i>cpxA</i>	CpxA of <i>K. aerogenes</i> G7 cloned into pBAD33	This study
pBAD33- <i>cpxA</i> ^{Y144N}	CpxA ^{Y144N} of <i>K. aerogenes</i> P4 cloned into pBAD33	This study
pBAD33- <i>cpxA</i> ^{R33C}	R33C site-directed mutagenesis from pBAD33- <i>cpxA</i>	This study
pBAD33- <i>cpxA</i> ^{T252P}	T252P site-directed mutagenesis from pBAD33- <i>cpxA</i>	This study
pACYC184	Tet ^r , Cm ^r ; Cloning vector	New England Biolabs
pACYC184- <i>ampRC</i>	AmpR and AmpC of <i>K. aerogenes</i> ATCC13048 cloned into pACYC184	This study
pET24a+	Kan ^r ; Expression vector, <i>P_{T7}</i> IPTG inducible	Novagen
pET24a+- <i>cpxA</i> His	CpxA of <i>K. aerogenes</i> G7 cloned into pET24a+ for overexpression in C41(DE3)	This study
pET24a+- <i>cpxA</i> *His	CpxA ^{Y144N} of <i>K. aerogenes</i> P4 cloned into pET24a+ for overexpression in C41(DE3)	This study
pET24a+- <i>cpxR</i> His	CpxR of <i>K. aerogenes</i> G7 cloned into pET24a+ for overexpression in BL21(DE3)	This study
pKNT25	Kan ^r ; Vector generating N-terminal fusion to T25	Euromedex
pUT18C	Amp ^r ; Vector generating C-terminal fusion to T18	Euromedex
pKT25- <i>zip</i>	T25- <i>zip</i> expression plasmid	Euromedex
pUT18- <i>zip</i>	T18- <i>zip</i> expression plasmid	Euromedex
pCpxA-SD-T25	CpxA-SD cloned into pKNT25	This study
pCpxA-SD*-T25	CpxA ^{Y144N} -SD cloned into pKNT25	This study
pUT18C-CpxP	CpxP cloned into pUT18C without its signal sequence	This study

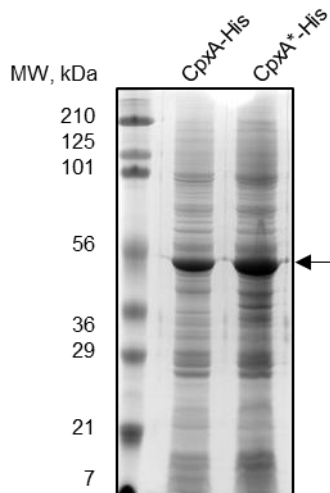
4



5

6 **Supplementary Figure 1. Purified CpxR-His after nickel affinity chromatography and**
7 **buffer exchange.**

8



9

10 **Supplementary Figure 2. Purification of inner membrane vesicles containing CpxA-His**
 11 **and CpxA*-His.**

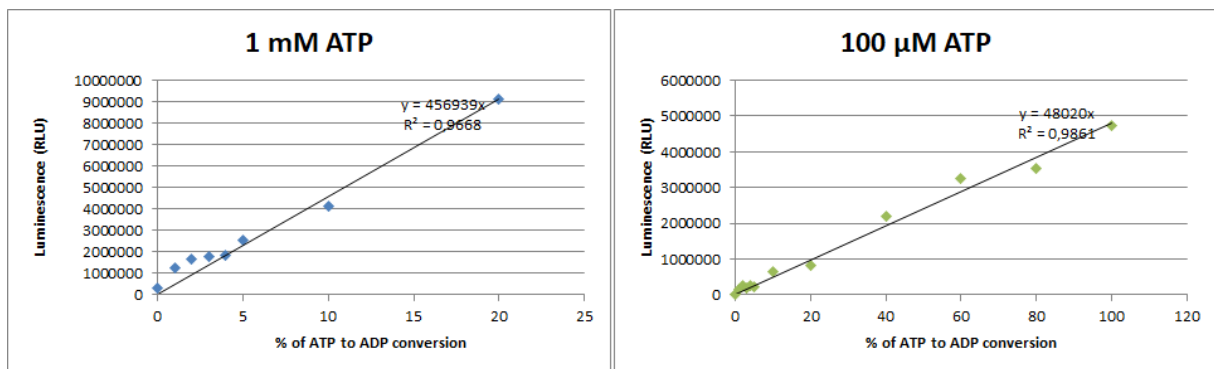
12

13 **ADP-Glo™ kinase assay**

14 The reactions were performed in a volume of 5 μ l, in the presence of 100 μ M or 1 mM ATP
 15 and incubated for 30 min at room temperature in a solid white 384-wells assay plate. Then, the
 16 assay is performed in two steps after completion of the kinase reaction: first, the ADP-Glo
 17 reagent is added that simultaneously terminates the enzyme reaction and removes remaining
 18 ATP; second, after 40 min incubation, the kinase detection reagent is added that converts ADP
 19 to ATP and simultaneously converts the generated ATP into light using luciferin/luciferase
 20 reaction. The amount of light generated is proportional to the ADP produced and the activity of
 21 the kinase. ATP to ADP standard curves were prepared in the phosphorylation buffer to assess
 22 the linearity of the assay order to calculate the amount of ADP produced from each reaction.
 23 The 1 mM ATP and ADP concentration range was created by mixing proportionally an amount
 24 of 1 mM ADP and 1 mM ATP in a microtiter plate to always reach a concentration of 1 mM
 25 total nucleotides. This 1 mM series (12 concentration points from 0 to 100% ATP or 100 to 0%
 26 ADP) was then diluted 1:10 to make the 100 μ M series. A volume of 5 μ l for each of the 12
 27 points was transferred to the assay plate and ADP-Glo reagents were added as follows: 5 μ l

28 ADP-Glo reagent was added then the plate was mixed for 30 s and incubated at room
29 temperature for 40 min. Then, 10 μ l of kinase detection reagent was added and the plate was
30 mixed again before incubating it for a minimum of 60 min to allow the highest concentrations
31 of ADP to fully convert to ATP and to be used by luciferase/luciferin reaction (**Figure S3**). For
32 both standard curves and assays, luminescence was recorded by using a TECAN $\text{\textcircled{R}}$ Infinite Pro
33 M200 instrument set to 0.5 sec integration time.

34



35

36 **Supplementary Figure 3. Linearity of the ADP-GloTM kinase assay for the 100 μ M and 1**
37 **mM ATP series.** Luminescence values represent the mean of 2 replicates. Abbreviation: RLU,
38 relative light unit.

39

40 **Phosphorylation of CpxR with acetyl phosphate**

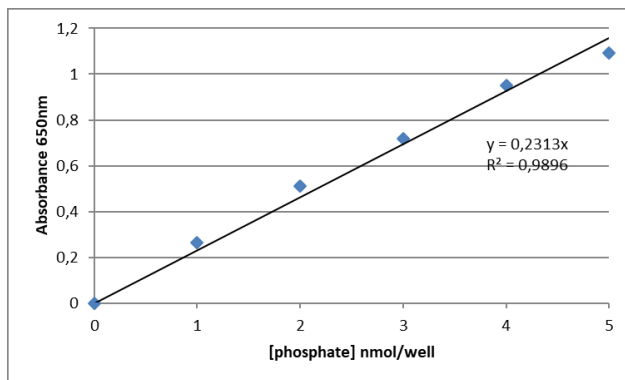
41 Acetyl phosphate was synthesized by mixing 2 units of acetate kinase (Sigma) with 500 μ M of
42 ATP diluted in 0.1 M triethanolamine buffer (pH 7.8) containing 10 mM K acetate, 1 mM
43 MgCl_2 , and 10% glycerol at room temperature for 2 h. The solution was then ultrafiltrated
44 through a Microcon Ultracel YM-10 filter (Millipore) at $14,000 \times g$ at 4°C for 30 min. Purified
45 CpxR-His (25 μ M) diluted in phosphorylation buffer was incubated with the ultrafiltrate (200
46 μ l), at room temperature for 30 min. The reaction mixture was transferred to a concentrator
47 (Vivaspin 500, 10,000 MWC0 PES, Sartorius) and centrifuged at $13,000 \times g$ for 5 min. After

48 discarding the filtrate, the concentrate was diluted in phosphorylation buffer and centrifuged
49 again. This procedure was repeated 3 times to remove free ATP and acetyl phosphate.

50

51 **Phosphate colorimetric assay**

52 Phosphate reacts (in standards and samples) with a chromogenic complex, which results in a
53 colorimetric product proportional to the amount of phosphate present (**Figure S4**). The assay
54 was performed in microplates and absorbance was measured at 650 nm using a TECAN ®
55 Infinite Pro M200 instrument.



56

57 **Supplementary Figure 4. Standards for colorimetric phosphate assay.** Absorbance values
58 represent the mean of a duplicate. 10 μ l of the 10 mM phosphate standard was with 990 μ l of
59 water to prepare a 0.1 mM phosphate standard solution. 0, 10, 20, 30, 40, and 50 μ l of the 0.1
60 mM phosphate standard solution were added into a 96 well plate, generating 0 (blank), 1, 2, 3,
61 4, and 5 nmole/well standards. Water was added to each well to bring the volume to 200 μ l. 30
62 μ l of phosphate reagent was added to each well. Mixtures were incubated for 30 min at room
63 temperature before readings.

64

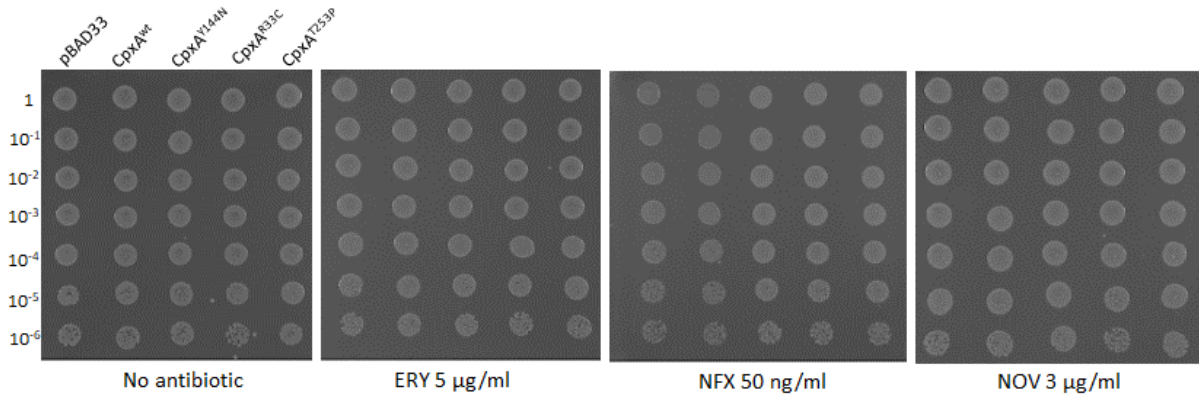
65

66

67

68

69 **Supplementary results**



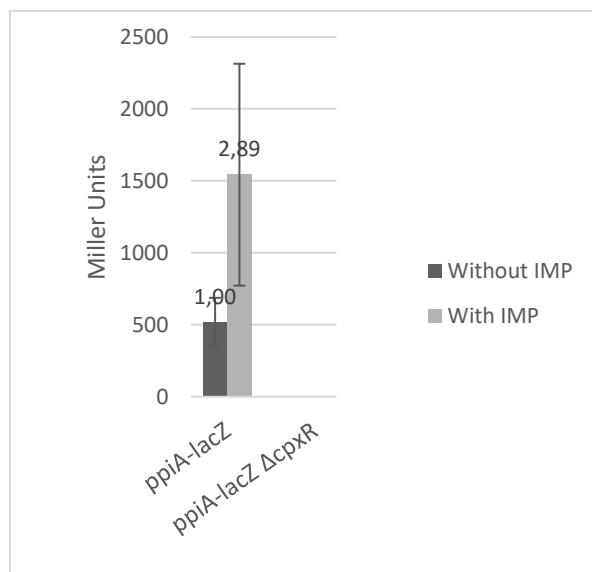
70

71 **Supplementary Figure 5. *cpx*^{*} alleles do not increase resistance macrolides,**

72 **fluoroquinolones or novobiocin.** EOP assays were performed as described in Materials and

73 **Methods.** ERY, erythromycin; NFX, norfloxacin; NOV, novobiocin.

74



75

76 **Supplementary Figure 6. The Cpx system is activated by imipenem. A *ppiA-lacZ***

77 **transcriptional fusion was used as a Cpx reporter activity.** The fusion was significantly activated

78 **(~2-3 fold) in the presence imipenem (0.32 µg/ml for 1 h @ 37°C) to level similar to that *cpxA*^{*}**

79 **alleles, but completely abolished in a *ΔcpxR* background.**

80

81

82 **Supplementary references**

- 83 1. Philippe N, Maigre L, Santini S, Pinet E, Claverie JM, Davin-Régli AV, Pagès JM, Masi
84 M. 2015. *In vivo* evolution of bacterial resistance in two cases of *Enterobacter aerogenes*
85 infections during treatment with imipenem. PLoS One 10:e0138828.
- 86 2. Casadaban MJ. 1976. Transposition and fusion of the lac genes to selected promoters in
87 *Escherichia coli* using bacteriophage lambda and Mu. J Mol Biol 104:541-555.
- 88 3. Werner J, Misra R. 2005. YaeT (Omp85) affects the assembly of lipid-dependent and lipid-
89 independent outer membrane proteins of *Escherichia coli*. Mol Microbiol 57:1450-1459.
- 90 4. Masi M, Duret G, Delcour AH, Misra R. 2009. Folding and trimerization of signal
91 sequence-less mature TolC in the cytoplasm of *Escherichia coli*. Microbiology 155:1847-
92 1857.
- 93 5. Gerken H, Charlson ES, Cicirelli EM, Kenney LJ, Misra R. 2009. MzrA: a novel modulator
94 of the EnvZ/OmpR two-component regulon. Mol Microbiol 72:1408-1422.
- 95 6. Denome SA, Elf PK, Henderson TA, Nelson DE, Young KD. 1999. *Escherichia coli*
96 mutants lacking all possible combinations of eight penicillin-binding proteins: viability,
97 characteristics, and implications for peptidoglycan synthesis. J Bacteriol 181:3981-3993.
- 98 7. Evans KL, Kannan S, Li G, de Pedro MA, Young KD. 2013. Eliminating a set of four
99 penicillin-binding proteins triggers the Rcs phosphorelay and Cpx stress responses in
100 *Escherichia coli*. J Bacteriol 195:4415-4424.
- 101 8. Datsenko KA, Wanner BL. 2000. One-step inactivation of chromosomal genes in
102 *Escherichia coli* K-12 using PCR products. Proc Natl Acad Sci U S A 97:6640-6645
- 103 9. Guzman LM, Belin D, Carson MJ, Beckwith J. 1995. Tight regulation, modulation, and
104 high-level expression by vectors containing the arabinose PBAD promoter. J Bacteriol
105 177:4121-4130.